The use of remote sensing to evaluate the effectiveness of soil and water conservation measures in the West Usambara Mountains, Tanzania

R.J.H. Masselink
3062066
27 November 2011

Universiteit Utrecht

The use of remote sensing to evaluate the effectiveness of soil and water conservation measures in the West Usambara Mountains, Tanzania

Universiteit Utrecht

Faculty of Geosciences
Department of Physical Geography

Msc Physical Geography
Thesis

27 November 2011

Supervisors
Dr. G. Sterk
Prof. Dr. S.M. de Jong

R.J.H. Masselink
3062066

Abstract

The highlands in Tanzania are seriously affected by soil erosion, which leads to the formation of gullies, the collapse of soil and water conservation measures and the loss of fertile topsoil, which in turn leads to a reduction of crop yields, food deficiency, silting-up of waterways, damage to structures and loss of land value. Over the course of the past century considerable efforts have been undertaken to reduce the amount of erosion by means of soil and water conservation measures, but only minimal adoption of the promoted measures has been achieved, making soil erosion an on-going problem.

The aim of this study was to locate soil and water conservation measures in the Usambara Mountains, Tanzania and to model their effectiveness. This was done by (1) assessing erosion risk in the entire Lushoto district, (2) locating soil and water conservation measures in two smaller, 10x10 km blocks near the villages of Soni and Sunga, (3) modelling the erosion in those blocks, and (4) model the effectiveness of the soil and water conservation measures.

An erosion risk map of the entire district was created by using a Landsat Enhanced Thematic Mapper+ (ETM+) image and a digital elevation model created from a contour lines map with a vertical resolution of 50m. Land use maps of the 10x10 blocks were created using two standard pixel-based methods and an object-based, nearest neighbourhood method on two different scale levels. The pixel-based methods that were used were a minimum distance to means and a maximum likelihood classification method.

The locations of bench terraces and grass strips were located by using object-based image analysis and the land use map with the highest accuracy, which in this case was the map created with the maximum likelihood classification method. This land use map was used to mask out areas that were not of interest. The percentage of agricultural area that contained soil and water conservation measures ranged from 2.9% to 19.75% for the Soni and Sunga blocks, respectively.

The Universal Soil Loss Equation was used to quantitatively assess the erosion in the 10x10 km blocks. Areas containing soil and water conservation measures had an average modelled soil loss of 39.82-51.96 t ha^{-1} yr^{-1}. The effectiveness of the soil and water conservation measures was modelled to be 42-58%.

Table of contents

1. Introduction

The most important land degradation problem worldwide is soil erosion by water (Eswaran et al., 2001). Soil erosion adversely affects the productivity of all natural ecosystems as well as agricultural, forest and rangeland ecosystems (Lal & Stewart, 1990; Pimentel, 1993; Pimentel et al., 1995; Pimentel & Kounang, 1998). Soil erosion is, together with the ever growing human population, water availability, energy and the loss of biodiversity one of the most pressing environmental problems in the world (Pimentel, 2005). A growing world population needs a growing amount of food. Of this food, 99.7% comes from land, while the remaining 0.3% comes from the oceans and other aquatic ecosystems (FAO, 1998). The productivity and quality of soils is therefore a key-factor in maintaining the world food supply.

Soil erosion occurs in a three-stage process: detachment -> transport -> deposition of the soil particles. Energy for these processes can be physical, chemical or anthropogenic (Lal, 2001). Erosion begins with the impact of raindrops, which cause splash detachment of soil particles. The main mechanisms of detachment are the disintegration of aggregates by slaking, cracking, dispersion and shearing by raindrop impact or run-off. Slaking results from compression of air entrapped inside rapidly wetted aggregates (Yoder, 1936; Hénin et al., 1958). Cracking results from differential swelling and shrinkage; dispersion results from the reduced cohesion between wetted colloidal particles (Le Bissonais, 1996). Shearing, as well as transport by splash and run-off, depend largely on kinetic energy of raindrops and run-off, but also on the properties of the soil itself (Casenave & Valentin, 1989). As run-off increases according to the length of the slope, it's shearing and transport capacities also increase, and erosion evolves from sheet erosion to more severe rill erosion (Roose, 1996).
These rills can then evolve into gullies, although their genesis is often more complex, involving sub-surface flows and side-wall processes (Bocco, 1991). This process of erosion by water is controlled by climatic characteristics, topography, soil properties, vegetation and land management.

One of the worst examples of a soil erosion problem is sub-Saharan Africa, where it negatively affects sustainable agricultural production (Lal, 1988). Yield reduction due to land degradation may be as much as 14.5% by the year 2020 (Lal, 1995). The highlands in Tanzania are seriously affected by soil erosion; as much as 100 t ha^{-1} of fertile topsoil may be lost annually, resulting in the formation of gullies, collapse of soil and water conservation measures, which in turn leads to a reduction of crop yields, food deficiency, silting-up of waterways, damage to structures and loss of land value (Pfeiffer, 1990; Shelukindo & Kilasi, 1993; Kaswamila, 1995; Lyamchai et al., 1998). Moreover, the

lower lying plains are also dependent on the rivers that originate in these mountainous areas for drinking water, irrigation of crops, etc.

The Usambara Mountains are part of the Tanzanian highlands, where erosion is an on-going problem (Conte, 2004: Johanson, 2001). Over the course of the past century considerable efforts have been undertaken to reduce the amount of erosion by means of soil and water conservation measures. Soil and water conservation measures protect the soil from splash and flow detachment. This is achieved by reducing the amount of soil exposed to direct impact of raindrops with e.g. mulching or agroforestry, or by reducing the runoff velocity by implementing e.g. grass strips or bench terraces. Also, measures like agroforestry increase interception, making relative direct throughfall of the precipitation smaller, resulting in a lower availability of water for overland flow. In the Usambara Mountains efforts for the implementation of soil and water conservation measures were first done by the German and British colonial rulers and afterwards by the Tanzanian government, but the adoption by famers of the promoted measures was only minimal, making soil erosion an on-going problem in these areas (Conte, 2004; Johanson, 2001).

Over the past years several studies have been conducted to assess the reasons for this minimal adoption of soil and water conservation measures in the Usambara Mountains and other areas in Sub-Saharan Africa (e.g. Tenge, 2005; Mowo et al., 2002). These studies however, were all conducted from a socio-economic point of view. The reasons for a minimal adoption could however also lie in (bio)physical aspects, that have yet to be studied in the area. In order to begin to understand why adoption of the soil and water conservation measures is only minimal, it is necessary to know where the current measures are located, and whether or not they are placed at locations where they would be expected, based on the (bio)physical properties of that location. In order to know where ideally the soil and water conservation measures should be placed in the landscape, erosion risk needs to be assessed.

Studies where erosion was quantitatively modelled with e.g. the WEPP model (Lane & Nearing, 1988) or the LISEM model (De Roo et al., 1994, 1996a, 1996b) have been numerous over the past two decades, but have only been done on field scale (e.g. Soto & Días-Fierros, 1997) or for small catchments up to 100 km^2 (e.g. Hessel, 2003), for which these models were designed. However, on a regional scale like Lushoto district, a simplification of e.g. the micro topography and local spatial variability in vegetation and soils becomes necessary, making the approach more qualitative. Because of the size of the area, remote sensing is a suitable tool to qualitatively assess erosion. Erosion risk can be estimated through combining a land use classification with slope characteristics

(e.g. Vrieling et al., 2006). Other studies assessing spatial erosion at the regional scale (50-10,000 km^2) include the application of erosion models in a GIS, such as the (Revised) Universal Soil Loss Equation (Blaszczynski, 1992; Mati et al., 2000; Šúri et al., 2002).

In order to give a general overview of the entire area and an idea of where vulnerable areas for erosion are located, erosion risk at district level needs to be known. Subsequently, in order to assess where soil and water conservation measures would ideally be placed, erosion risk mapping on a smaller (block) scale needs to be done. To be able to assess the measure of adoption of soil and water conservation (SWC) measures and relate that to the erosion risk in the area it is necessary to locate where the measures are already in place. The SWC measures are clearly visible on high resolution satellite imagery, suggesting that it is possible to extract these with an automated process, as was done for other features in the landscape by e.g. Addink & Kleinhans (2008) and Van der Werff & Van der Meer (2008). For the extraction of the SWC measures the relatively new technique of Object-based Image Analysis (OBIA) could prove useful, while instead of using only spectral information of single pixels as is done with pixel-based classifications, shape information can also be taken into account with this method.

Object-based image analysis uses objects to classify different features in an image rather than a more general pixel-based approach. An algorithm is used to create segments (objects), which are regions that are generated by one or more criteria of heterogeneity. These segments have additional spectral information compared to single pixels (e.g. mean values per band, median values, minimum and maximum values, mean ratios, variance etc.), but of even greater advantage than the diversification of spectral value descriptions of objects is the additional spatial information for objects (Blaschke & Strobl, 2001; Darwish et al., 2003; Flanders et al., 2003; Benz et al., 2004; Van der Werff and Van der Meer, 2008; Hay and Castilla, 2008). In order to map the soil and water conservation measures with the highest accuracy, it is necessary to exclude areas that by definition do not have these measures (e.g. forests and built-up areas). These areas can be excluded using a land use map of the entire study area. The additional spectral and spatial information obtained with object-based classification image analysis methods would imply that these methods are superior to pixel-based methods for e.g. land use classifications (Blaschke, 2010). In order to determine whether this was the case for the study area, several pixel-based and object-based methods were compared to each other.

The overall aim of this study was to locate soil and water conservation measures in the district of Lushoto, Tanzania, to link these locations to the erosion risk in the area and estimate their effectiveness against soil erosion by water. Furthermore a comparison was made between 'traditional' pixel-based classification methods and object-based classification methods.

The main goals for this study were:

1. To assess the differences in accuracies between pixel-based and object based land use classification methods.
2. To map the locations of soil and water conservation measures in the study area with the highest possible accuracy.
3. To qualitatively model soil loss and to estimate the effectiveness of the soil and water conservation measures in the study area.

In order to achieve these goals, next to the analysis of remotely sensed data on two scales (district and block scale), field work was done in the study area of the Lushoto district, Tanzania. The main aim for the field work was to get general knowledge of the vegetation, soils and land use in the area, to determine locations and characteristics of different types of soil and water conservation measures and to collect data for an accuracy assessment.

2. Remote sensing methods

Remote sensing has several applications in the study of erosion; erosion features like rills or gullies can be mapped using remotely sensed imagery (Vrieling et al., 2007), while erosion risk can be derived from remote sensing products (Vrieling et al., 2006; Sonneveld, 2003).

Erosion controlling factors e.g. topography, soils and vegetation can be mapped using remote sensing. For topography, digital elevation models (DEMs) can be extracted from e.g. stereo optical imagery (Toutin & Cheng, 2003). Important factors on the basis of which soils can be classified include soil properties, climate, vegetation, topography and lithology, which can potentially be mapped by remote sensing (McBratney et al., 2003). Vegetation can be mapped in several ways, e.g. using vegetation indices (Lillesand et al., 2004) or (un)supervised classification methods (e.g. Feoli et al., 2002; Jürgens & Fander, 2003).

In the following paragraphs first some basic satellite remote sensing principles and two pixel-based classification methods that were used in this study will be described in short. Secondly, the recent method 'Object-based image analysis' (OBIA) and its classification methods will be explained in detail.

2.1 Basic satellite remote sensing principles and applications used in this study

Satellite sensors record electromagnetic radiation, which is subsequently transmitted to the ground where it is stored in electronic form. Radiation can be measured at different wavelengths, e.g. visible light and infrared. This recorded radiation needs to be processed in order to obtain useful information. The data can be processed with e.g. pixel-based or object-based classification methods. Variables obtained from satellite data may subsequently be combined with additional spatial data to extract new or more accurate information (e.g. He et al., 1998; Lubczynski & Gurwin 2005).

Satellite imagery needs to be corrected for e.g. changes in scene illumination and atmospheric conditions in order to perform quantitative analyses (Lillesand et al., 2004). In some cases, *radiometric correction* will be performed by the supplier of the image, in other cases, like freely available data (e.g. Landsat TM data) the data have to be radiometrically corrected by the user.

Raw digital images usually contain geometric distortions so significant that they cannot be used directly as a map base without subsequent processing (Lillesand et al., 2004). These distortions can be divided into random and systematic distortions. Systematic distortions are easily corrected by applying formulas derived by modelling the sources of the distortions mathematically. Random distortions are less predictable and include

changes in relief and atmospheric refraction. These distortions can be overcome by using either ground control points, or in case of relief displacement a digital elevation model (Lillesand et al., 2004).

Some satellite sensors (e.g. ASTER) have the capability of making *stereo images*, because they use two telescopes; one *nadir* looking (directly downward) and another looking backward, which is 27.7° off nadir in the case of ASTER. In this way, stereoscopic images can be produced, with which it is possible to create digital elevation models (DEM's) with a vertical accuracy of 7-50m for the ASTER sensor (Lillesand et al., 2004).

The data which is recorded by the sensor can be displayed in multiple ways, of which the *image space* is the most used way to project the data. Another display method is called the *feature space* in which reflectance values of the pixels of two or more bands are put in a scatter plot, with which it is for instance possible to distinguish different land use types. Examples of an image space and a feature space are given in figure 2.1.
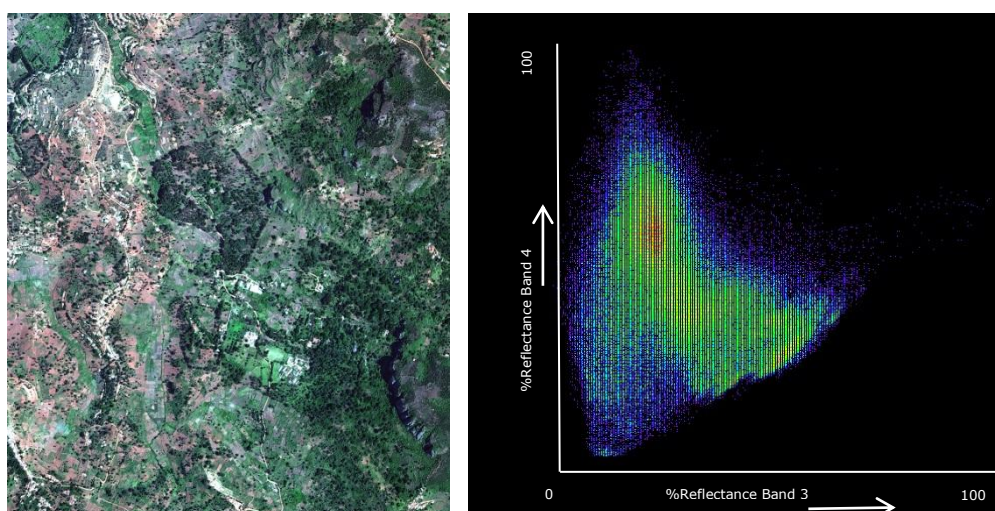
Figure 2.1 Examples of an image space (left) and a feature space (right).

Sensors often have the capability to record data of relatively high resolution in a panchromatic band, of which the resolution is two (Landsat ETM+) to four (e.g. Worldview-2, Quickbird) times higher than the other visible and near-infrared bands. With this panchromatic band it is possible to enhance the resolution of the other image bands using algorithms like the Gram-Schmidt algorithm (Laben & Brower, 2000) or a principal component transformation (Welch & Ahlers, 1987).

Vegetation indices can be used to study the amount of (healthy) vegetation present in the image area. A good example of a vegetation index is the *Normalised Difference*

Vegetation Index (NDVI), which calculates a ratio between the reflectance (ρ) values of the red and near-infrared (NIR) band (Lillesand et al., 2004).

$$NDVI = \frac{\rho(NIR) - \rho(red)}{\rho(NIR) + \rho(red)} \tag{1}$$

Because the NDVI is an image ratio, it reduces the effect of topography, meaning that it overcomes differences in incoming solar radiation (Holben and Justice, 1981).

In order to determine what kind of remotely sensed image to obtain, or to what scale different objects can be studied on a certain image, it is necessary to understand which model the user is dealing with. An H-resolution model is defined as one in which the elements in the scene are larger than the resolution cells; the L-resolution model presents the opposite case (Woodcock et al., 1986). The terms *high* and *low* are avoided because they tend to be associated with absolute measurement scales rather than the relative size of elements. An example of an H-resolution model would be a house on an image with a pixel size of 50 cm, while an example of an L-resolution model would be that same house on an image with a pixel size of 50 m. In this study that means that in order to obtain an H-resolution model, the pixel size of the image must be smaller than the extent of the soil and water conservation measures.

2.2 Pixel-based land use classification methods and accuracy assessments

The terms land use map and land cover map are often used interchangeably, while this is not correct. Land cover is determined by direct observation while land use requires socio-economic interpretation of the activities that take place on that surface (Fisher et al., 2005). An example of a land cover type is forest, and for that land cover type multiple land use types could apply, e.g. natural forest or planted forest for lumber. Often a combination of land use and land cover is used, which was also the case for this study. Maps that were derived in this study will be referred to as land use maps to prevent confusion. Land use maps can be derived from land cover maps, which in turn can be classified from satellite imagery using a number of methods. Of these methods, two will be described in this paragraph, as well as general principles to take into account when classifying land use. Also a method to determine the accuracy of the proposed classification methods will be described.

Per-pixel classification methods can generally be divided into *supervised* and *unsupervised classification methods*. Supervised classification methods require the user to "supervise" the process by selecting inputs for the method, and therefore the user also has influence over the results. In an unsupervised classification the different classes

are automatically grouped together, without interference of the user. As only supervised classification methods were used in this study, only these will be described.

In a supervised classification process, the user goes through three basic steps; the (1) training stage, (2) classification stage and (3) output stage (Lillesand et al., 2004).

The overall objective of the training stage is to assemble a set of statistics that describe the spectral response pattern for each land cover type to be classified in an image (Lillesand et al., 2004). This is achieved by selecting training areas that represent the land cover types that the user wants to classify. It is commonly accepted that the minimum amount of pixels for these training areas should be $n+1$ pixels, with n being the number of spectral bands of the sensor. In practice, a minimum of $10n$ to $100n$ is used, as this improves classification accuracy (Lillesand et al., 2004).

In the classification stage a method for classifying the different land cover types needs to be chosen. Two examples of these classification methods are the 'minimum distance to means' classifier and the 'maximum likelihood' classifier.

The *minimum distance to means* classification method calculates the distances between the spectral values of the pixels for each band in the image and the means of the different land cover types (or training areas) in each band. The pixels are assigned the class to which the distance is the smallest (Lillesand et al., 2004). This principle is depicted in figure 2.2.
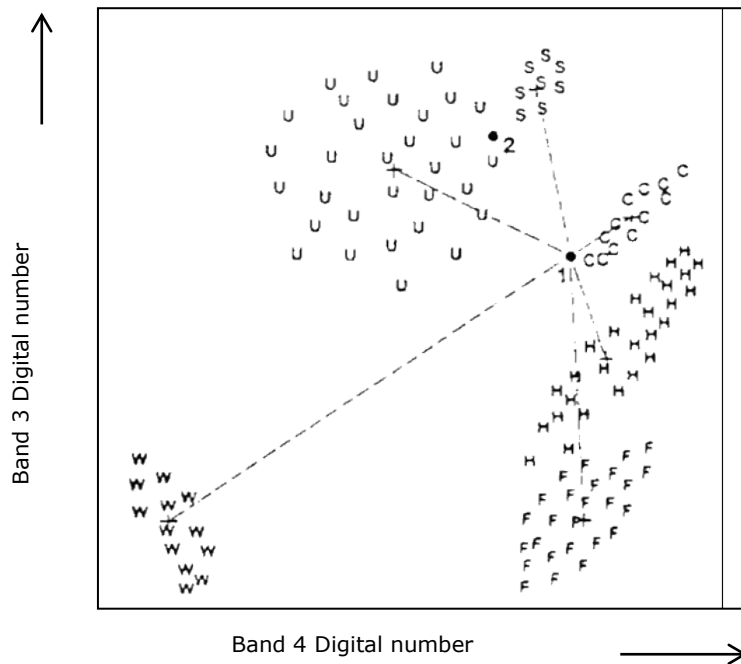
Figure 2.2 Minimum distance to means classification method. The class of which the mean has the shortest distance to the target pixel (with number 1) will be assigned to the target pixel. In this case the pixel would be classified as C (corn). Pixel 2 would we classified as being S (sand).

The *maximum likelihood classifier* assumes that the distribution of the cloud of points in the forming the category training data is normally distributed, which is a reasonable assumption for common spectral responses. The method computes the statistical probability of a certain pixel being a member of a particular land cover class (Lillesand et al., 2004). Figure 2.3 depicts the principle of a maximum likelihood classification.
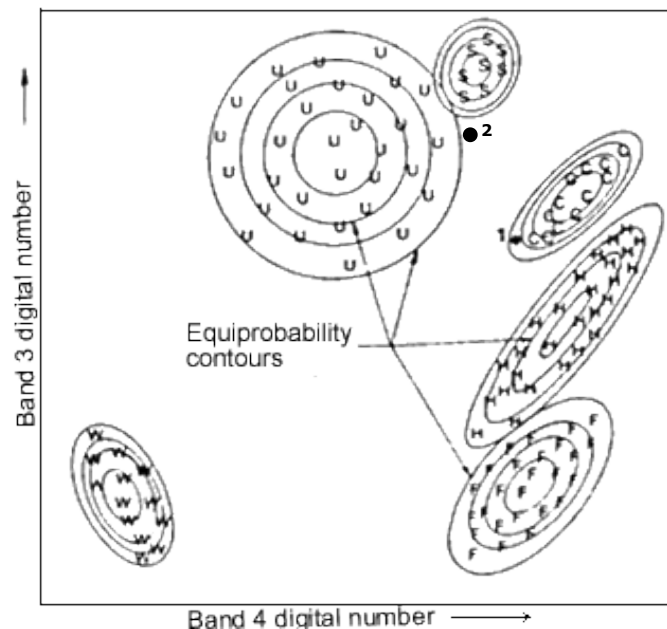

Figure 2.3 Maximum likelihood classification method. Equiprobability contours for each class are calculated and the class to which the target pixel is most likely to belong to is assigned to the pixel. In this case the target pixel (with number 1) is assigned as C (corn), number 2 is assigned as U (urban).

A 'salt-and-pepper' pattern is common after applying a per-pixel classifier, which is due to small scale spatial and spectral variability. The pattern can be (partly) removed using a *majority filter*, which replaces cells in a raster based on the majority of their contiguous neighbouring cells (Figure 2.4).
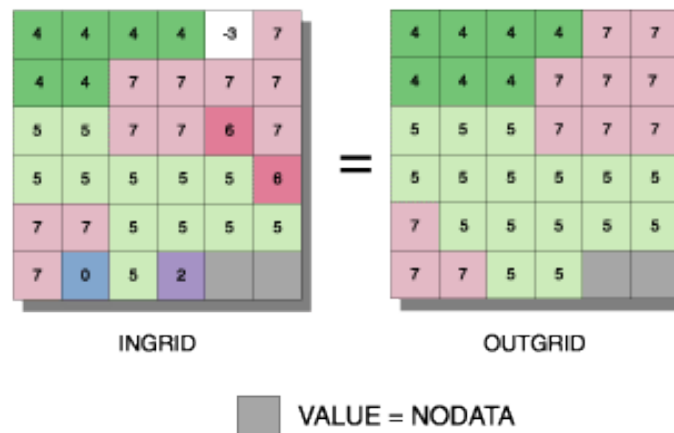

Figure 2.4 The principle of a 3x3 majority filter. From a target pixel, the values of 8 neighbouring cells are evaluated and the target pixel value will be adjusted accordingly (ArcGis 10 manual, Esri).

In order to assess the accuracy of the classification at the output stage, an accuracy assessment needs to be done. One of the most common means of expressing classification accuracy is het preparation of a *classification error matrix*. Error matrices compare, on a category-by-category basis, the relationship between known *reference data* (ground truth data) and the *classification data* (Lillesand et al., 2004). From these error matrices an overall accuracy, as well as a user's accuracy and a producer's accuracy can be extracted. The user's accuracy indicates the probability that a pixel that is classified into a given category actually represents that category on the ground. The producer's accuracy indicates how well training set pixels of the given cover type are classified (Lillesand et al., 2004).

2.3 Object-based Image analysis

Object-based Image Analysis (OBIA) entails creating objects (clusters of pixels) in an image space. An algorithm is used to create objects, which are regions that are generated by one or more criteria of heterogeneity in one or more dimensions, respectively (Blaschke and Stroble, 2001). These objects can be created with a number of different algorithms; in this case a segmentation algorithm in the software programme eCognition (version 8.64, Trimble, München, Germany) was used. In this programme, the segmentation algorithm is a bottom-up region-merging technique starting with one-pixel objects. In numerous subsequent steps, smaller image objects are merged into bigger ones. In each step, the pair of adjacent image objects that would result in the smallest growth of the defined heterogeneity is merged. If the smallest growth exceeds

the threshold defined by the scale parameter, the process stops (Benz et al., 2003). The scale parameter can be set by the user, depending on the application and the needs of the user.

The step-wise segmentation process as described by the eCognition reference book (version 8.64, 2010) is:

1. The segmentation procedure starts with single image objects of one pixel and repeatedly merges them in several loops in pairs to larger units as long as an upper threshold of heterogeneity is not exceeded locally. This heterogeneity criterion is defined as a combination of spectral heterogeneity and shape heterogeneity (eq.2). A scale parameter was set by the user to determine the general size of the objects. Higher values for the scale parameter result in larger image objects, smaller values in smaller image objects.
2. As the first step of the procedure, the seed (object) looks for its best-fitting neighbour for a potential merger.
3. If best fitting is not mutual, the best candidate image object becomes the new seed image object and finds its best fitting partner.
4. When best fitting is mutual, image objects are merged.
5. In each loop, every image object in the image object level will be handled once.
6. The loops continue until no further merger is possible.

eCognition considers shape and colour to be the primary object features (Benz et al., 2003) and therefore the change in heterogeneity, which is the determining factor for the merging of objects, is defined as:

$$\Delta h = w_{colour} * \Delta h_{colour} + w_{shape} * \Delta h_{shape} \qquad (2)$$

$$w_{colour} + w_{shape} = 1$$

where:

Δh = Change in heterogeneity of an object

w_{colour} = User defined weight for colour ($w_{colour} \in [0,1]$)

Δh_{colour} = Change in spectral heterogeneity (eq.3)

w_{shape} = User defined weight for shape ($w_{shape} \in [0,1]$)

Δh_{shape} = Change in shape (eq.4)

The change in spectral heterogeneity Δh_{colour} is defined as:

$$\Delta h_{colour} = \sum_{c=1}^{m} w_c \left(n_{merge} * \sigma_{c,merge} - \left(n_{obj1} * \sigma_{c,obj_1} + n_{obj2} * \sigma_{c,obj2}\right)\right) \tag{3}$$

Where:

c	= Image band number
m	= Total number of image bands
w_c	= A factor that can be added to give more weight to one or more image bands
n_{merge}	= The number of pixels in the merged object
$\sigma_{c,merge}$	= The standard deviation within the merged object
n_{obj1}	= The number of pixels of object 1 before merging
n_{obj2}	= The number of pixels of object 2 before merging.

The change in shape (Δh_{shape}) describes the improvement of the shape with regard to smoothness and compactness, which are the most important characteristics to determine shape (Benz et al., 2003).

This change in shape is defined as:

$$\Delta h_{shape} = w_{comp} * \Delta h_{comp} + w_{smooth} * \Delta h_{smooth} \tag{4}$$

$$w_{comp} \in [0,1], \; w_{smooth} \in [0,1], w_{comp} + w_{smooth} = 1$$

with

$$\Delta h_{smooth} = n_{merge} * \frac{l_{merge}}{b_{merge}} - \left(n_{obj1} * \frac{l_{obj1}}{b_{obj1}} + n_{obj2} * \frac{l_{obj2}}{b_{obj2}}\right) \tag{5}$$

$$\Delta h_{comp} = n_{merge} * \frac{l_{merge}}{\sqrt{n_{merge}}} - \left(n_{obj1} * \frac{l_{obj1}}{\sqrt{n_{obj1}}} + n_{obj2} * \frac{l_{obj2}}{\sqrt{n_{obj2}}}\right) \tag{6}$$

Where:

l	= The perimeter of the object
b	= The perimeter of the object's bounding box (figure 2.5)

The bounding box of an object is the smallest rectangular area that encloses all pixels of the object (figure 2.5). The bounding box is therefore defined by the minimum and maximum values of the x and y coordinates of an image object (eCognition reference book 8.64, 2010).
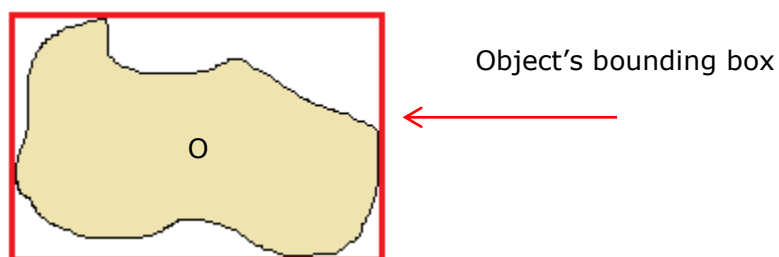
Figure 2.5 An object (O) and its bounding box

The weights w_c, w_{color}, w_{shape}, w_{comp} and w_{smooth} are weights that can be defined by the user to allow for the best segmentation results, depending on the considered application (Benz et al., 2003).

Next to having spectral characteristics, as do pixels, the objects that are formed during the segmentation process also contain shape characteristics. These characteristics can be used in mapping land use or mapping separate features e.g. buildings, landmarks or naturally occurring features such as river meanders (Addink and Kleinhans, 2008). An object which is made up out of a stretch of road has significantly different shape characteristics than an object which is made up out of a house. The eCognition software is able to use this additional shape information in a nearest neighbourhood classification where the user can determine which spectral and/or shape information should be included in the classification. This nearest neighbourhood classification is implemented by selecting a number of samples (training areas) that are representative for a certain class. Certain shape and spectral characteristics can be assigned to these samples and be given a certain weight according to the needs of the user. A class is assigned to each object in the image space by finding its nearest neighbour in the group of samples, according to its spectral and shape characteristics.

3. Study area

The Usambara Mountains are located in northeast Tanzania within latitudes 4° 05' to 5° 00'S and longitudes 38° 05' to 38° 40'E and consist of two parts; the Eastern and Western Usambara's respectively, which are separated by the Lwengera Valley. The study will focus on Lushoto district (figure 3.1), which comprises almost 70% of the entire West Usambara Mountains area (Mowo et al., 2002).
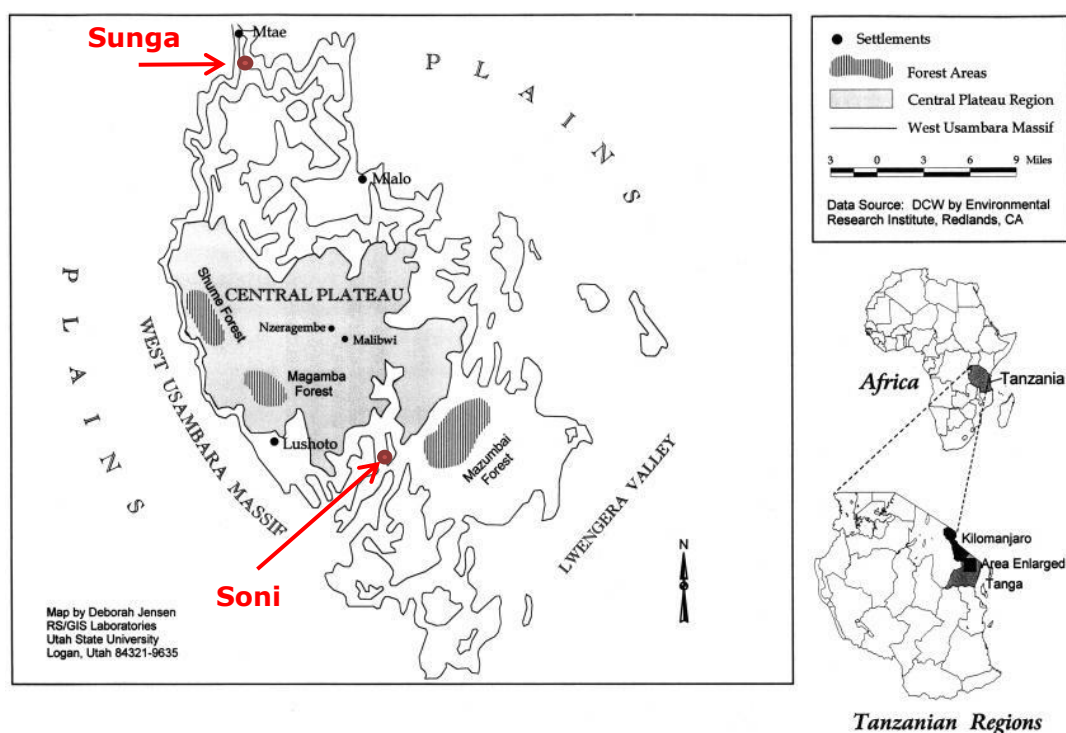

Figure 3.1 The location of the Usambara Mountains, Tanzania and the Soni and Sunga study areas. The Lushoto district corresponds roughly with the 'West Usambara Massif' in the figure (Conte, 1999).

Block level

Two smaller areas of 10*10 km within Lushoto district have been studied in more detail. These are the areas around the villages of Soni and Sunga (figure 3.1). These areas were chosen for their large difference in adoption of soil and water conservation measures. The Soni area has very little adoption of soil and water conservation measures, while the adoption of these measures in the Sunga area is much better. Another main difference between the two areas is that the Sunga area has relatively more forested area than the Soni area, 18% and 6% respectively. Also, part of the Sunga area consists of steep ridges sloping downward onto the plains below.

Only the Soni area was used for fieldwork and a smaller subset area in the 10x10 km block was chosen for the development of the classification methods. This was done to reduce calculation times and for logistic reasons. The subset area near Soni is shown in

figure 3.2. In the northwest of the image the southern part of the Soni village is visible, in the west of the image, just south of the Soni village lies the Shashui village. In the northeast and southeast some large rock outcrops can be seen. Mainly the western part of the area is used for agriculture, where in the eastern part also some forest is present. This subset area was chosen because it has a high diversity in land use and in the occurrence of soil and water conservation measures.
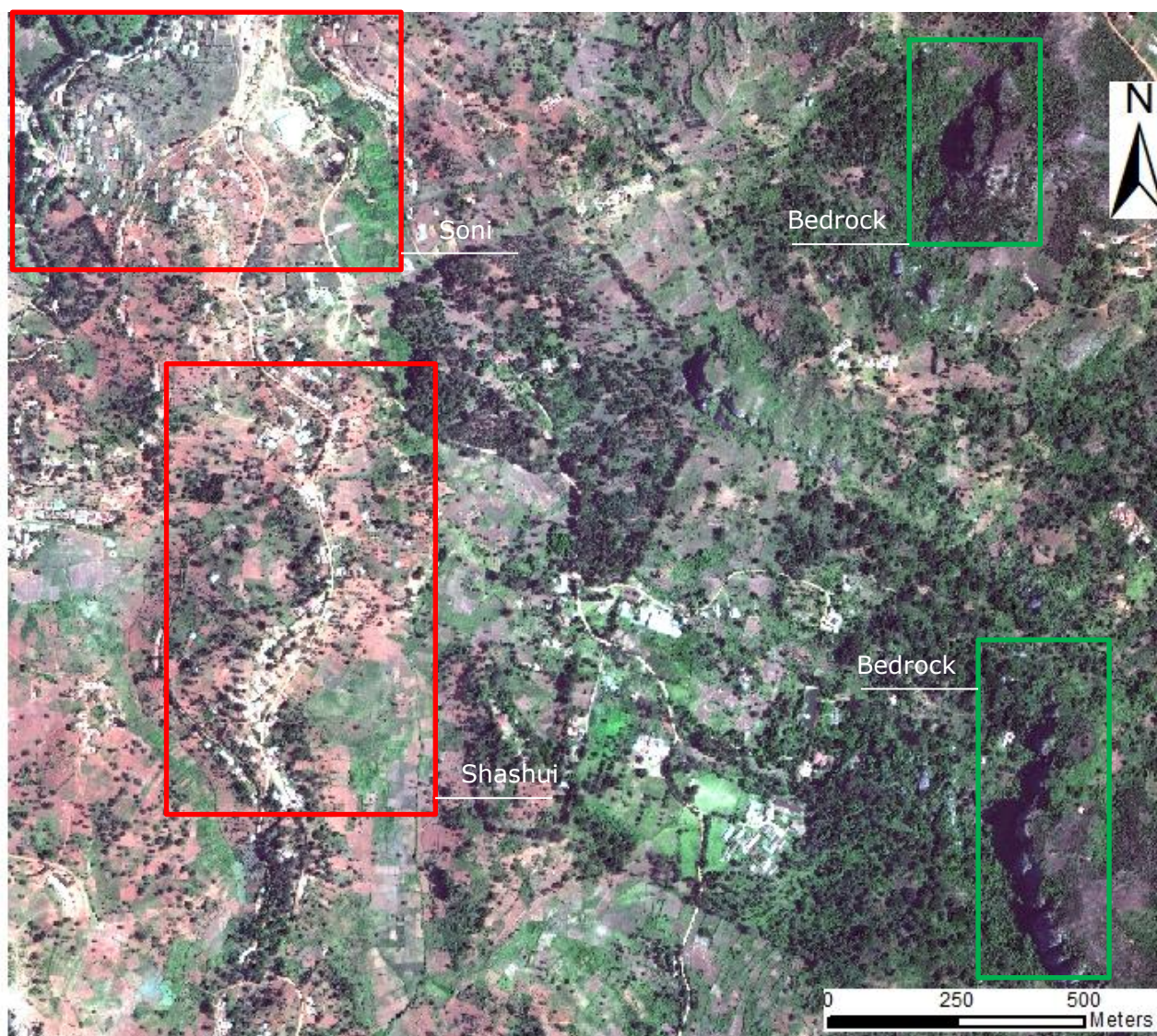

Figure 3.2 The subset study area near Soni, Tanzania. The villages of Soni and Shashui are depicted, as well as two bedrock outcrops.

Topography and geology

The substrate in Usambara mountains consists of Precambrian metamorphic rocks, mainly gneisses, hornblendes and schists, which were uplifted during the Tertiary, approximately 65 million years ago (Geological Survey Tanzania, 1965). The mountain plateau reaches to an altitude of 2350 m a.s.l., while the surrounding plains have an altitude of approximately 600 m a.s.l. There is a considerable relief in the mountains with steep slopes. The drainage pattern follows a number of fault-controlled troughs, mainly running N-S and NNW-SSE. The stream valleys are mainly V-shaped (Geological Survey Tanzania, 1965). In the study areas of Soni and Sunga the elevation ranges between 900-1800 m and 750-2350 m respectively. Both areas are highly dissected with slopes up to 90%.

Climate

Rainfall is bimodal and falls mainly in March-May and in September-November in the locally named long and short rains, respectively. The average yearly precipitation ranges between 800-1700 mm. These large differences are mainly caused by topography (Pfeiffer, 1990). Highest rainfall is found on the sea-facing south and south-east slopes (Lundgren, 1978). Depending on altitude and season, average maximum temperatures range between 20 °C and 25 °C, where average minimum temperatures range between 10°C and 15 °C (Figure 3.3)

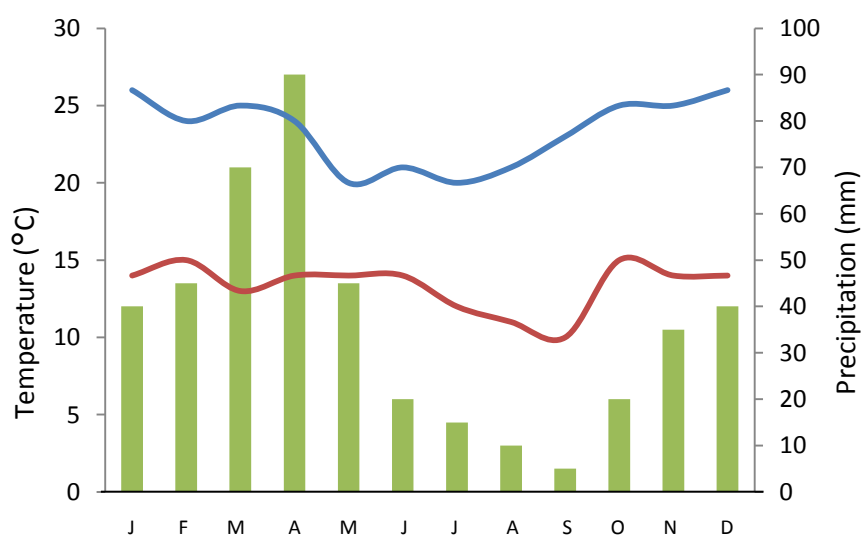Figure 3.3 Average minimum (red line) and maximum (blue line) temperatures and monthly average rainfall for Soni, Tanzania (edited from Heijnen, 1974).

Soils

The soils in the area are Humic and Haplic Acrisols on the slopes and ridges, Haplic Lixisols on the footslopes and Eutric Fluvisols and Umbric Gleysols in the valleys (Vrieling et al., 2006) The soils in Lushoto district have a high clay content (table 3.1), but due to

formation of sand sized water-stable aggregates, they have good drainage characteristics (Sanchez, 1976; Lundgren, 1980).

Soil texture data of 16 points in both the Soni and Sunga blocks were gathered and analysed. The average texture values and organic carbon percentages are depicted in table 3.1.The soils in the Soni area generally have higher clay content, and a lower sand content than the Sunga block.

Table 3.1 Soil characteristics, averages for the Soni and Sunga blocks.

Location	%Clay <2 μm	%fine silt 2-20 μm	%course silt 20-50 μm	%Sand 50-2000 μm	Organic carbon %
Soni	40	9.35	6.32	44.65	2.31
Sunga	28.29	11.5	5.5	55.29	3.24

Vegetation

In the Soni block the majority of the indigenous vegetation has been removed in order to create space for agricultural practices. In the southeast of the area some 6 km^2 of natural forest still exists. In the Sunga area approximately 10 km2 is natural forest and another 8 km2 is planted forest (pine), used for lumber.

The crops that are cultivated range from cabbage in the valleys to an intercropping system of maize, cassava, beans, sugar cane and banana on the slopes. In some relatively small areas tea and coffee is cultivated. Just before the start of the rain seasons the fields are ploughed and prepared for sowing, making the fields vulnerable to erosion. High intensity rainfall falls unimpeded on the soil, where mulch of the previous harvests has been removed. Survey results done by Tenge (2005) showed that fields with maize and beans are most prone to erosion.

Soil and water conservation measures

Soil and water conservation measures that are common in African highlands include bench terraces, grass strips, fanya juu and agroforestry (Tenge, 2005). Bench terraces consist of a series of level or nearly level platforms along the contour lines of the slope at suitable intervals. Bench terraces are recommended for slopes between 35% and 55% (Shelukindo, 1995). Fanya juu are hillside ditches of which the excavated soil is placed upslope from the ditches. The ditches intercept surface runoff by breaking the slope into multiple segments. Fanya juu are common on slopes between 12-35%. Grass strips consist of different grass species planted in strips along the contour lines and are

generally placed on slopes between 5-12%. Grass strips ensure a reduction in flow velocity, in turn causing sediment to settle. Agroforestry refers to a land use practice where perennial trees are integrated with crops and in some cases animals in the same field. Tenge (2005) measured the effectiveness of these measures in the Usambara Mountains, of which the results are shown in table 3.2.

Table 3.2 Effectiveness of SWC measures in reduction of soil loss and surface runoff in the Usambara Mountains, Tanzania (Tenge, 2005).

Slope Class *	SWC	Soil loss (Mg/ha)	Surface runoff (M^3/ha)	Effectiveness	
				Soil loss (%)	Surface runoff (%)
Moderate	Control	4.8	1.14	0	0
	Agroforestry	0.1	0.12	98	89
	Fanya juu	0.1	0.06	99	95
Steep	Control	9.7	0.84	0	0
	Grass strips	0.4	0.24	96	71
Very steep	Control	12.8	2.34	0	0
	Bench terraces	0.2	0.13	98	94

* Moderate (13-25%), Steep (26-35%), Very steep (>55%)

Soil and water conservation measures that are implemented in the study area of Soni include bench terraces, strips of Napier grass (Pennisetum purpureum), strips of Guatemala grass (Tripsacum laxum) and different forms of agroforestry (Shelukindo, 1995; AHI, 2000; Semgalawe, 1998; Liversage, 1994). Fanya juu measures are absent in the Soni block. The soil and water conservation measures in the Sunga block mainly consist of bench terraces.

4. Data and methods

4.1 Field data

During a three month period from September to December 2010, just before and during the 'short rains', field work was carried out to obtain general knowledge of topography, soils, vegetation and land use of the Soni study area. For the error analyses of the classification methods ground truthing data were collected. Also an attempt was made to assess erosion risk and quantitatively measure erosion. During the fieldwork period however, there was no precipitation in the study areas, making the measurements of erosion impossible.

Topography

The Soni area is highly dissected with steep slopes and narrow valley floors.

Agricultural fields can be found on steep slopes of up to 68%, which was the highest measured slope on which agriculture was present (Figure 4.1). In this particular case no soil and water conservation measures were present except for mulching.

Figure 4.1 Maize field with a slope of 68 % in the Soni subset study area.

Ground-Truthing

The land use of 250 points in the Soni area was assessed. These points were used as reference data in the accuracy assessment of the pixel-based and object-based land use classification methods (paragraph 4.7).

Soil and Water conservation measures

The soil and water conservation measures that were present in the area included bench terraces, grass strips, mulching and agroforestry. The size of the different SWC measures is an important feature in deciding whether or not the resolution of the satellite imagery is sufficient, i.e. the model has an L-resolution or H-resolution. Dimensions of the grass strips and bench terraces were measured at 29 different sites in the Soni area. The minimum and maximum values are depicted in table 4.1.

Table 4.1 Measured minimum and maximum dimensions of bench terraces and grass strips in the Soni study area.

Measure	Height (m) Min-max	Width(m) Min-Max	Length (m) Min-Max
Grass strips	0.1-0.4	7 – 20	15-180
Bench terraces	0.3-0.6	1.5-4	10-65

4.2 Maps and Satellite Imagery

Data available for this study comprise: a Landsat Enhanced Thematic Mapper + (ETM+) (NASA, USA) image of 25 October 1999, a Worldview-2 (WV-2) (Digitalglobe, Longmont, CO, USA) and a digital elevation model extracted from an ASTER (NASA, USA) image. The satellite data and the corresponding sensor characteristics are depicted in table 4.2. An example of the ETM+ and WV-2 images that were used can be seen in figure 4.3.

Table 4.2 Sensor and image characteristics of satellite imagery used in this study

Sensor	Spatial resolution	# of spectral Bands	Spectral domain	Image date	Remarks
ETM +	15 m (pan)	1	VNIR	25 October,	Some clouds visible in the south of
	30 m	6	VNIR, SWIR	1999	the district
	60 m	1	TIR		
ASTER	15 m	3	VNIR	2005	Only used for input to create a
	30 m	6	VNIR, SWIR		DEM
	90 m	5	TIR		
Worldview-2	0.46 m (pan)	1	VNIR	30 January,	Sunga image: some cloud cover in
	1.64 m	3	VNIR	2010	the north and east

The Landsat Enhanced Thematic Mapper+ (ETM+) image was taken in October 1999, which normally means the end of the dry period or the beginning of the 'short rains', of which the timing and amount of precipitation is less reliable and predictable than the 'long rains'. With both options however, vegetation on agricultural fields is minimal. The Worldview-2 image was taken on the 30th of January, which means that more vegetation was present, as crops have grown considerable. Field work was carried out after a dry

spell of nearly four months, which meant that the vegetation cover was significantly less than at the acquiring date of the Worldview-2 image, but corresponds well to the conditions of the acquiring date of the ETM+ image.

4.3 Scale levels

Two scale levels were used to assess erosion risk at different spatial levels. The highest scale level is the district level, which comprises the entire district of Lushoto, approximately 3500 km^2. The block level includes two areas of 100km^2 around the villages of Soni and Sunga respectively. At the district level the erosion risk was assessed, of which the methods and results can be found in appendix I. Also at the district level soil and water conservation measures were mapped and the classified images were used in the quantitative mapping of erosion at the block levels. Figure 4.2 shows a summary of the two scale levels, the data which were used and the products which were produced at those levels. Figure 4.3 depicts images of the two different scale levels.
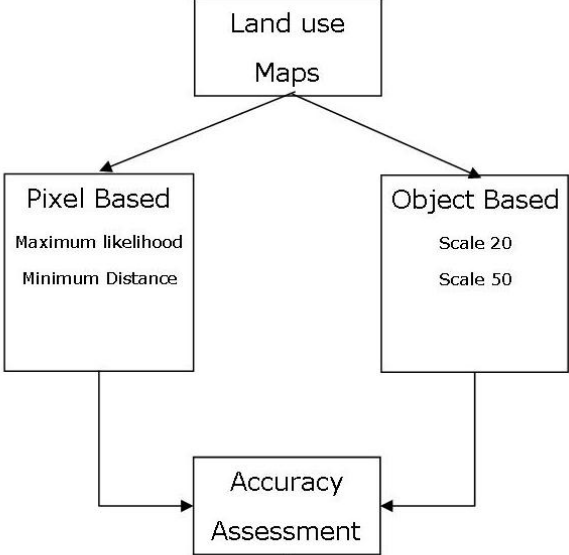
Level	Product	Data
District Level	Erosion risk Map (Appendix I)	ETM+ Image DEM from con-tour lines
Block Level	Land use Maps → Pixel Based (Maximum likelihood, Minimum Distance) / Object Based (Scale 20, Scale 50) → Accuracy Assessment	Worldview-2 Image
Block Level	SWC Map	Worldview-2 Image
Block level Erosion risk	Erosion Risk Map USLE	Worldview-2 Image Soil Data Weather Data DEM (ASTER)

Figure 4.2 Summary of the scale levels and derived products in this study

Figure 4.3 Two scale levels of the study. (a) District level (RGB=321) (b) Digital Elevation model at the district level (c) Block level (RGB=321) (d) Detailed view of the Block level (RGB=321)

4.4 Pixel-based land use classification

Before classifying the Worldview-2 images, they were pan-sharpened using the Gramm-Schmidt algorithm (Laben & Brower, 2000) in ENVI (ITT, Boulder, CO, USA). This was done to ob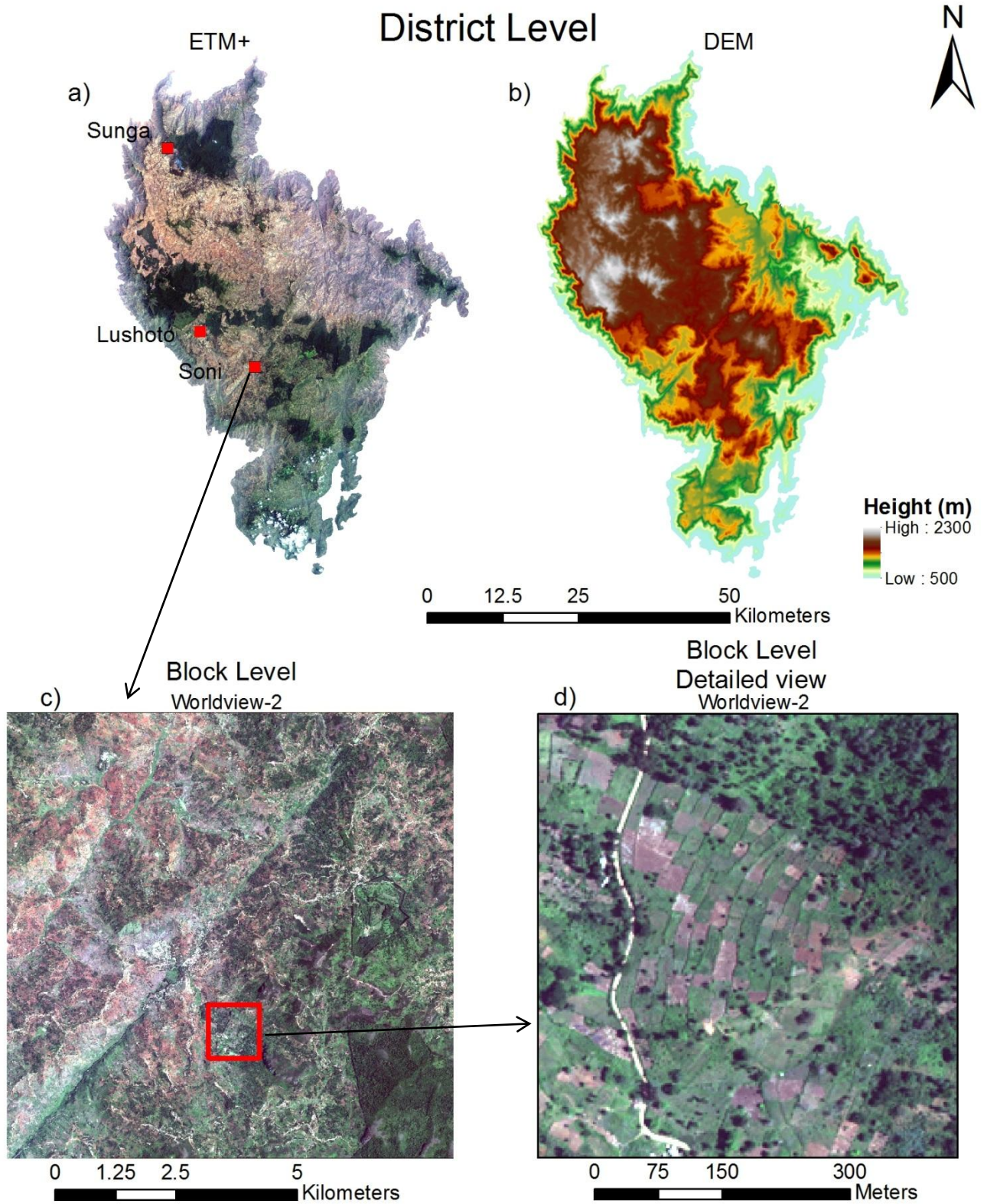tain an H-resolution model for the soil and water conservation measures with the smallest dimensions (table 4.1). For classification of land use, two supervised, pixel-based classification methods were used; the 'minimum distance to means' and the 'maximum likelihood' classifiers. In the training stage, 5 land use classes were created with a number of subclasses (figure 4.4). No more than 5 classes were chosen as trial-and-error proved that classification became less accurate by including more classes, which was probably due to the difference in timing of the image and the field campaign. Training areas were selected visually and based on field knowledge. All of the training areas for the subclasses contained at least 1000 pixels, which is sufficient for a supervised classification (Lillesand et al., 2004).
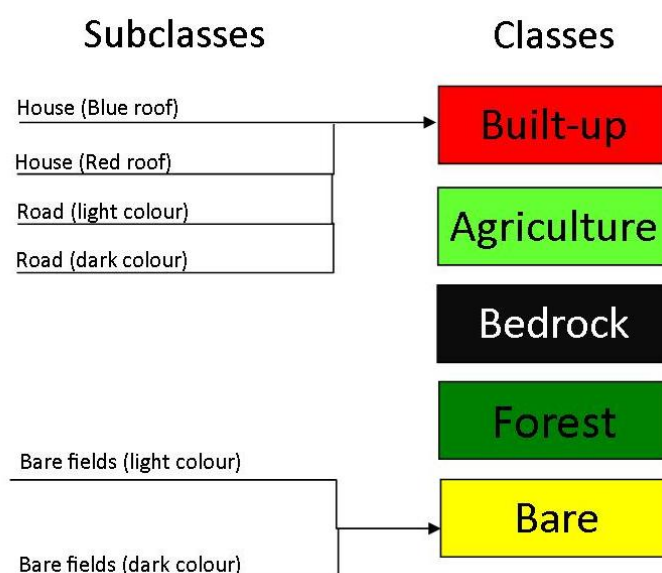
Figure 4.4 Five classes (right) and their subclasses(left) used for the land use classification of the Soni and Sunga study areas.

After the application of the classification methods, the subclasses were combined into the 5 main land use classes for a better comparison with each other and the object-based land use classifications. To remove the salt and pepper pattern which usually occurs in a pixel-based classifier, a 3x3 majority filter was used to smooth the results.

4.5 Object-based land use classification

As there is no standard, straightforward way to determine the best weights for image segmentation in an object-based land use classification, a trial-and-error method was used. The best segmentation weights were selected visually by comparing the size of the segmented objects to the size of the features in the image e.g. roads, houses and fields. As these features differ greatly in smoothness and compactness, i.e. a house and a road,

the compactness/smoothness was set to 0.5 which ensures an equal weighing. Two different values for the scale factor were used, the first was set to 50; this ensures single houses to be recognized as single objects and in some cases two or more objects. Setting the value higher causes houses to cluster into a single object, which is undesirable for the land use map, because there might be other land use types in between the houses. The second scale factor was set to 20, which causes objects from scale level 50 to be divided into several sub-objects. The difference in object size can be seen in figure 4.5.

For classification of the segmented objects, a nearest neighbour classification was applied. Twenty samples per land use class were visually selected. These samples were optimised using the *feature space optimisation* function in *eCognition* and where necessary, more samples were added.

An advantage of this object-based method over pixel-based methods is that next to spectral information also shape information can be included in the analyses. Objects that are elongated e.g. roads, can be more easily distinguished this way. An additional advantage over pixel-based methods is reclassifying pixels that have been classified wrongly. In this way shadow effects that occur in high resolution imagery can be reduced. In addition of using the spectral responses of the objects for classification, also the density of the objects was taken into account. The density of an object describes the distribution in space of the pixels of an image object. The shape with the highest density is a square; the more an object is shaped as an elongated feature, the lower its density (eCognition reference book, 2010). The density was added because objects that are made out of roads or segments of roads have a relatively low density, while houses have a high density and are therefore easily distinguishable on the basis of shape. As agricultural fields and forests have irregular shapes, these are difficult to classify with shape characteristics, and therefore these were mainly classified using their spectral response.

Figure 4.5 Segmentation results of part of the study area near Soni. Scale level 50 (top) and scale level 20 (bottom) are depicted.

Because of the high resolution of the Worldview-2 data, shadows are clearly visible in the image. Because of this shadow effect, different spectral responses occur where land use types are similar. This in turn could cause objects to be classified incorrectly. Using Object-based image analysis there is however a way to distinguish between land use types in shadows. With the aid of e.g. the NDVI, shadows can be distinguished from one another, as spectral indices like the NDVI remove the shadow effect. For this reason, the NDVI was used to reclassify shadows in the classified images.

In the image of the Sunga area some clouds are present. These clouds hinder the classification of the underlying land. Clouds are easily distinguishable spectrally due to their high water content (Lillesand et al., 2004), making reflection in all bands high. Therefore, a separate 'clouds' class was created in the Sunga area. This clouds class was omitted in the classification of SWC measures.

4.6 Error analyses of the land use classifications

The classification results of the two pixel-based and two object-based methods were compared to each other visually and by using error matrices. Error matrices have been created using 250 random sample points in the subset area of Soni. These points were randomly chosen in order to represent the relative land use of the entire area. The 250 random sample points were visually classified on the image. Points that could not be classified visually on the image were visited in the field to ensure a complete coverage of all the sample points.

4.7 Soil and water conservation measure detection using object-based image analysis

Before erosion risk could be mapped or modelled in the area, the location of soil and water conservation measures had to be surveyed because these reduce the volume of runoff and soil erosion. Visual inspection of the imagery revealed that bench terraces and grass strips can easily be identified in the high resolution Worldview-2 images. The successful visual identification may imply that object-based methods can also be successfully applied to map and identify land protection measures.

Certain areas were masked out from the analysis because no soil protection measures are applied in these areas. These areas comprise built-up areas, flat areas and areas with slopes steeper than 70%. The flat areas and steep slopes were not masked out of the process as the ASTER digital elevation model with a spatial resolution of 30m proved to be of too low accuracy to achieve this goal. The land use map with the highest classification accuracy was used to mask out built-up areas and bedrock.

The land use map with the highest classification accuracy was used as a *thematic layer* in the first segmentation stage, which ensured that object borders were formed along the built-up and bedrock areas, which made it easier to mask these areas out of the next analysis steps. A large scale parameter was applied in this first segmentation step, in order to create relatively large objects, which can easily be classified on basis of land use aided by the land use map. The built-up areas and the areas that consist of bedrock could be masked out at this level, after which segmentation and classification could continue at smaller scale levels. Subsequently, smaller scale levels were evaluated visually to determine at which scale level individual fields were distinguishable. In order to be able to classify the soil and water conservation measures even smaller scale levels were used.

The elevation drops in the fields containing grass strips and bench terraces were classified by using the difference in spectral response in respect to their neighbouring objects. The mean difference to neighbouring objects in spectral response in band 1 (blue) was calculated, as differences are the highest in this band due to its short wavelength. The 'mean difference to neighbouring objects' of all objects was calculated and the best threshold value for the classification of the elevation drops was visually selected.

Once the elevation drops of the SWC measures were classified, the fields in which they are positioned were given the class of 'SWC measures'. This was done by assigning the class 'SWC measures' to all the fields that contained a certain relative area of these elevation drops. The threshold for this relative area was also visually selected.

An accuracy assessment was made after classifying the SWC measures. This was done by randomly selecting 50 objects out of the classified image that have been classified as containing SWC measures and 50 objects that have been classified as "non-SWC" areas. Random numbers were assigned to all the objects in the image and the first 50 objects containing SWC measures and the first 50 objects without SWC measures were selected. These objects were used as reference data and classified as being an area with or without measures visually from the Worldview-2 image and in cases where this was not possible, field visits were made. As this was not possible for the Sunga block, new random objects were chosen in the case of an uncertain classification.

4.8 Erosion risk mapping with the Universal Soil Loss Equation

To assess the quantitative risk of erosion in the two 10x10 blocks, erosion risk maps were created. The maps were created using the Universal Soil Loss Equation (Wischmeier & Smith, 1978), which predicts the long-term average annual erosion rate

on a field slope based on rainfall pattern, soil type, topography, crop system and management practices. The model is empirical, developed on *unit plots* which have a uniform length-wise slope of 9 percent and are 72.6 feet (22.1 m) long.

The Universal Soil Loss Equation (USLE) is:

$$A = RKLSCP \tag{7}$$

Where:
A = Erosion loss	(t/ha/year)	
R = Rainfall and runoff factor	(MJ.mm/ha.hr.year)	
K = Soil erodibility factor	(t/ha)	
L = Slope length factor	(-)	
S = Slope steepness factor	(-)	
C = Cover and management factor	(-)	
P = Support practice factor	(-)	

The inputs for the USLE were derived from rainfall data, soil data, the WV-2 image, the DEM, and the soil and water conservation map created by Object-based Image Analysis.

The rainfall and runoff factor R

The R-factor is the sum of individual storm EI-values for a year averaged over long time periods (> 20 years) to accommodate apparent cyclical rainfall patterns. The *EI* term is an abbreviation for energy multiplied by the maximum rain intensity in 30 minutes (Renard and Freimund, 1992). As there is only data available from one year (2010) on an hourly basis, a different method was used to determine the R factor.

Lo et al. (1985) established that the R-factor was a valid erosivity index for Hawaii and chose average annual rainfall as the best estimator of average annual R. Up to 90% of the total spatial variation in the R-factor could be explained by variations in mean annual rainfall (P in cm). The equation is defined as:

$$R = 38.46 + 3.48P \tag{8}$$

Where:
R = Rainfall and runoff factor	(MJ.mm/ha.hr.year)	
P = Mean annual rainfall	(cm)	

To obtain values for R in this study, precipitation data from two weather stations was available on an hourly basis for the year 2010. For the Soni area the precipitation of 2010 summed up to be 680.2 mm, which means the R value for the area is 275.16. In the Sunga area the total precipitation summed up to 518.4 mm, which means an R factor of 218.46.

The Soil erodibility factor K

The soil erodibility factor k has been calculated through the following equation proposed by Lal & Elliot (1994):

$$k = 2.8 * 10^{-7} * M^{1.14} * (1.2 - a) + 4.3 * 10^{-3} * (b - 2) + 3.3 * (c - 3) \qquad (9)$$

Where:　　　　M = The particle size parameter, defined as:

$$M = (silt(\%) + sand(\%)) * (100 - clay(\%))$$
(10)

　　　　　　a = The percentage of organic matter

　　　　　　b = The code number defining the soil structure, ranging from 1(very fine granular to 4(massive or lattice)

　　　　　　c = The soil drainage class, ranging from 1(fast) to 6(very slow)

Soil texture data and organic matter content data at 16 different locations throughout the two blocks were available to establish the M factor (table 3.1). The soil structure and drainage class were set to the average values of 2 and 3, respectively. The K values calculated at these 16 positions were then interpolated for the entire block using inverse distance weighing to create a map of the erodibility factor for the entire block.

Slope steepness and Slope length factor LS

The slope angle and slope length factor LS is the expected ratio of soil loss per unit area from a field slope to that from a 22.1 m length of uniform 9% slope under otherwise identical conditions (Wischmeier & Smith, 1978).

The factors L and S were determined using the DEM of the two areas. This was done with the method developed by Moore et al. (2002). The slope (in degrees) and the flow accumulation for each cell were calculated. The LS factor is then determined by:

$$LS = \left(\frac{flowacc * area\ of\ cell}{22.13}\right)^{0.4} * \left(\frac{Sin(Slope)}{0.0896}\right)^{1.3} * 1.4$$

(11)

Where: LS= Slope and slope length factor   (-)
     flowacc = The number of upslope cells

In areas with bench terraces however, there is a different relationship as the slope length is different in those areas. Due to the construction of terraces the slope length can change from several hundreds of meters to just 1 meter. Therefore the areas where SWC measures have been classified, the flow accumulation was set to 1. As in the mapping of the soil and water conservation measures in this study the bench terraces and grass strips were combined into a single class, the slope length factor of areas with grass strips was also affected.

The DEM is the limiting factor in this erosion risk mapping, as it has a pixel size of 30 m where the rest of the maps have a resolution of 0.5 m. This means that the eventual erosion map also has a cell size of 30 m.

Cover and Management factor C

The cover and management factor C is the soil loss from land cropped under specific conditions to the corresponding loss from clean-tilled, continuous fallow (Wischmeier and Smith, 1978). As no extensive work was done on the determination of the cover factor in the entire area, it was not possible to accurately determine the C factor. Previous studies have shown that a correlation exists between the C factor and the NDVI of satellite imagery (De Jong, 1994). Therefore it was assumed that the lowest NDVI value for bare soil is comparable with a C factor of 1 and that the highest value for the NDVI (full canopy) is comparable with a C factor of 0. With these assumptions the relation between the NDVI and the C factor and with values for NDVI of 0.95456 and 0.2012 for the highest and lowest, respectively, the following relation exists:

$$C = -1.3274 * NDVI + 1.2671$$

(12)

Where: C   = Cover and Management factor   (-)
     NDVI = Normalised Difference Vegetation Index   (-)

Using this equation, a C factor map of the area was created. The lowest C values of 0 were set to 0.001 to avoid multiplication by 0 in the USLE equation (eq. 7).

The support practice factor P

The support practice factor describes the ratio of soil loss with a specific support practice to the corresponding loss with up-and-down slope culture (Wischmeier & Smith, 1978). The support practice factor was set to 1 where no SWC measures were used and to 0.5 where SWC measures are present. These values correspond with the values used for contour stripping (Wischmeier and Smith, 1978). Both the support practice factor P and the slope length factor L were changed in areas where soil and water conservation measures were present, where normally the changes in soil loss due to the construction of terraces would be calculated using a combination of the slope length factor L and the support practice factor P, while changes in soil loss due to the construction of grass strips would be calculated by only changing the support practice factor P (Wischmeier & Smith, 1978).

The different USLE factors were collected in a GIS and quantitative erosion risk was calculated per pixel. A maximum erosion value of 100 t ha^{-1} yr^{-1} was set in order to remove unrealistic erosion values occurring because of a slope factor which becomes too dominant. Erosion values were first calculated without the incorporation of soil and water conservation measures. The erosion risk was then compared to the actual location of soil and water conservation measures to be able to assess whether or not the measures are in locations where they would be expected. After this, the soil and water conservation measures were added to the USLE calculations and the difference in soil loss and the modelled effectiveness of the soil and water conservation measures was assessed.

5. Results

5.1 Land use classification of the Soni area

The four land use classification methods were applied to the Worldview-2 image of the Soni area of which the results are depicted in figure 5.1. The original, natural colour WV-2 image of the images in figure 5.1 is depicted in figure 3.2. It can be clearly seen that the different methods produce different results. The pixel-based classifiers (A & B) show more shadows classified as bedrock than the object-based methods. The built-up areas also have a different distribution throughout the different methods, with the maximum likelihood method having the largest built-up area, while the minimum distance to means method has the smallest area classified as built-up. The minimum distance to means classifier classifies more areas as being bare, while the maximum likelihood method classifies it as agriculture. The Object-based methods are somewhat in between the two concerning the classification of agricultural, bare soil and built-up areas.
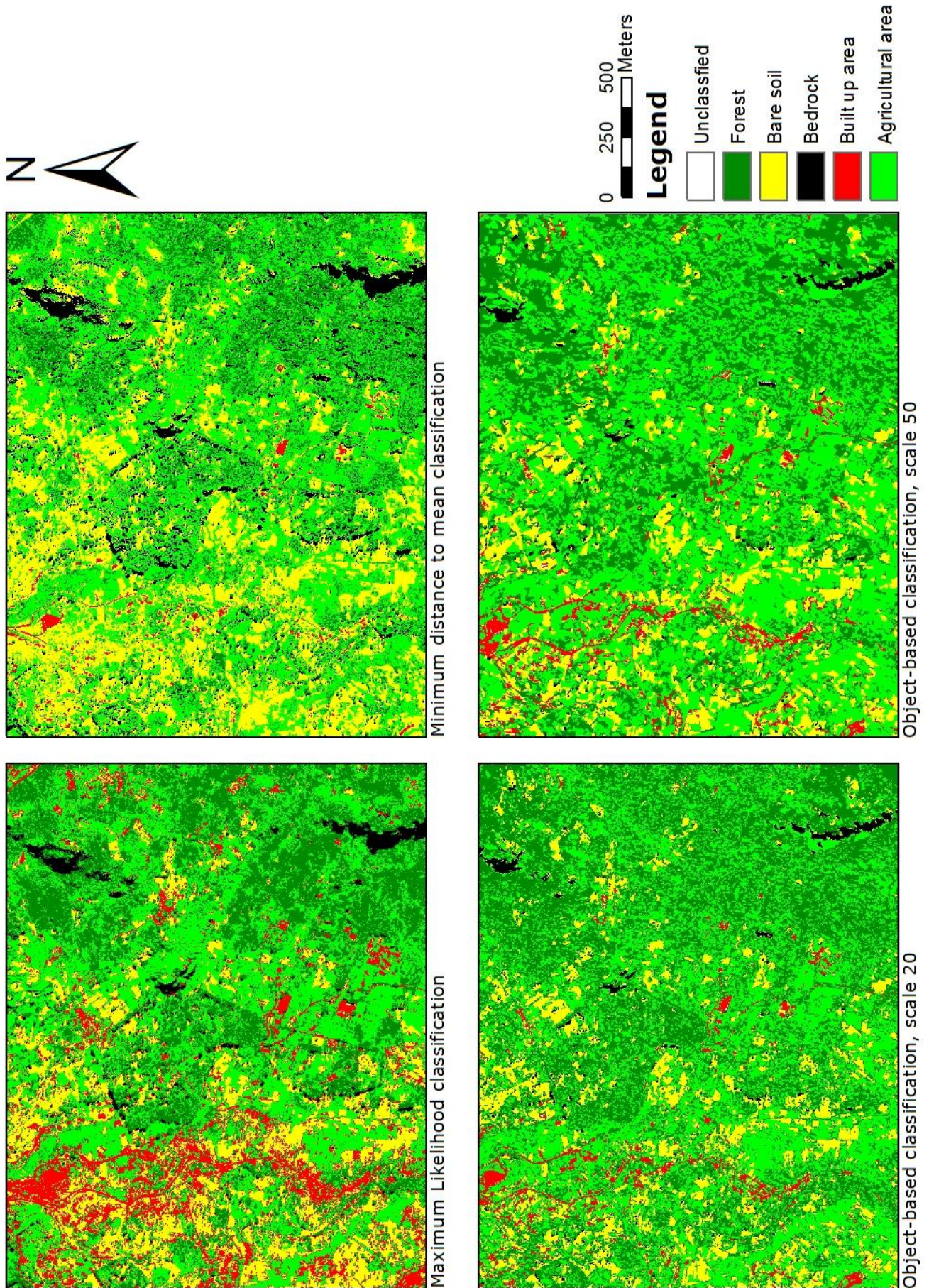
Figure 5.1: Four different land use classification methods for a part of the study area of Soni, Tanzania.

Universiteit Utrecht

Figure 5.2 shows the differences in classification results of the two object-based classification methods. It can be seen that the method using scale level 50 classifies more areas as built-up and forest than the method using scale level 20. The method using scale level 20 also classifies narrow roads, which are not classified in the scale level 50 classification.
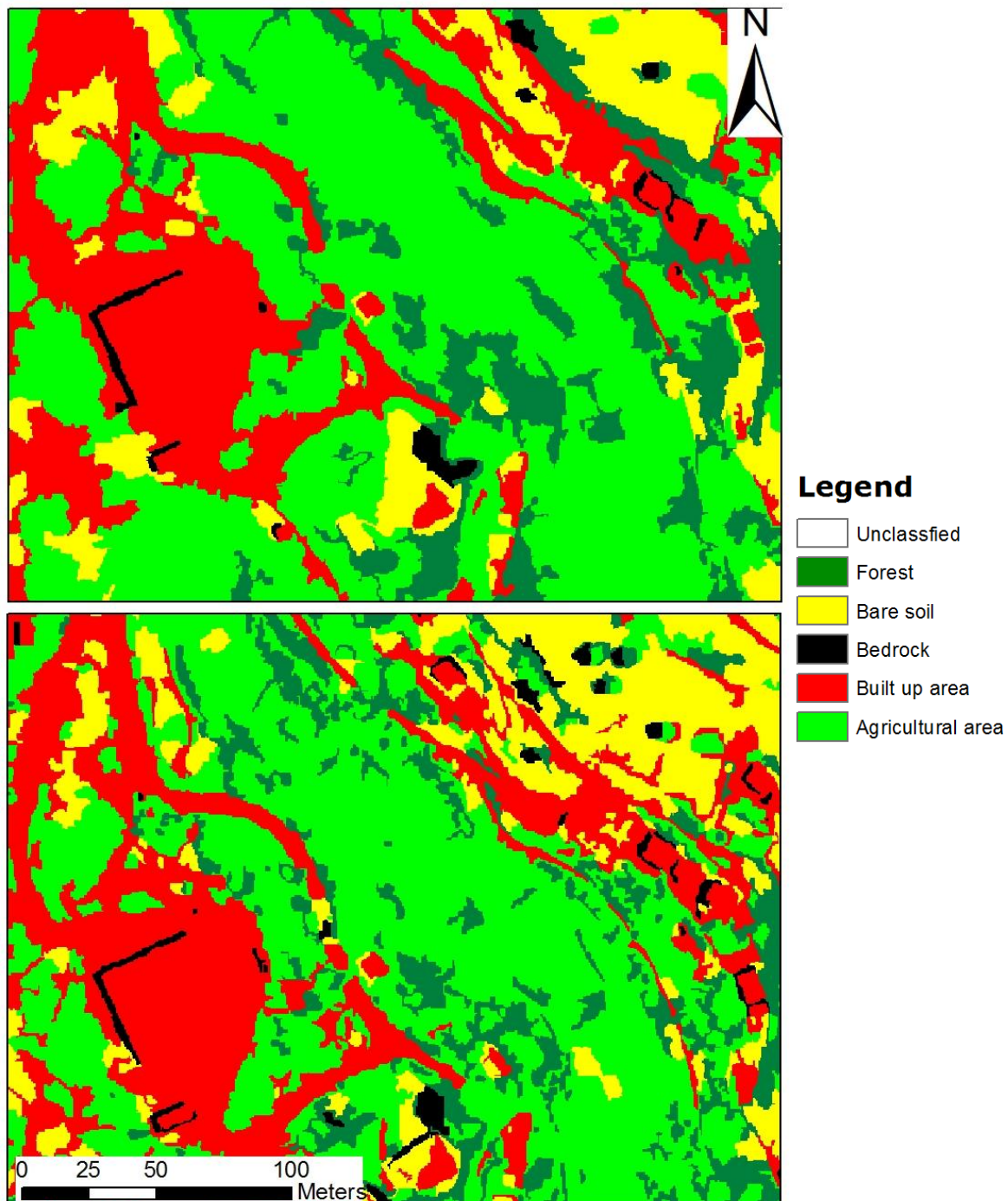
Figure 5.2: Object-based classifications of part of the study area near Soni, showing the differences between scale levels 50 (top) and 20 (bottom). For a natural colour image of the area see figure 4.5.

5.1.1 Accuracy assessment

The results of the accuracy assessments are depicted in the error matrices in table 5.1 Average accuracy values range from 42.97% for the Object-based classification method with scale factor 20, to 52% for the maximum likelihood classification. The accuracies for the land use types which are the most interesting, bare and agriculture are higher. The producer's accuracy for the 'bare' land cover class is for all methods low, which is due to an underestimation of the amount of bare pixels by all methods.

Table 5.1: Error matrices for four different land use classification methods for the subset study area near Soni.

Maximum Likelihood

Class name	Reference totals	Classified totals	Number correct	Producers Accuracy	Users Accuracy
Built-up	11	34	6	54.55%	17.65%
Bedrock	4	8	3	75%	37.50%
Bare	106	26	26	24.3%	100%
Agriculture	64	118	51	79.69%	43.22%
Forest	65	64	44	67.69%	68.75%
Overall Classification Accuracy					**52%**

Minimum Distance to means

Class name	Reference totals	Classified totals	Number correct	Producers Accuracy	Users Accuracy
Built-up	11	2	2	18.18%	100%
Bedrock	4	17	4	100%	23.53%
Bare	106	63	52	49.06%	82.54%
Agriculture	64	124	39	60.94%	31.45%
Forest	65	44	24	36.92%	54.55%
Overall Classification Accuracy					**48.40%**

OBIA-20

Class name	Reference totals	Classified totals	Number correct	Producers Accuracy	Users Accuracy
Built-up	11	9	5	45.45%	55.56%
Bedrock	4	3	2	50.00%	66.67%
Bare	106	25	25	23.81%	100%
Agriculture	64	132	44	68.75%	33.33%
Forest	65	80	31	47.69%	38.75%
Overall Classification Accuracy					**42.97%**

Table 5.1 (continued)

OBIA-50

Class name	Reference totals	Classified totals	Number correct	Producers Accuracy	Users Accuracy
Built-up	11	5	4	36.36%	80%
Bedrock	4	3	2	50%	66.67%
Bare	106	28	26	24.53%	92.86%
Agriculture	64	133	47	73.44%	35.34%
Forest	65	81	34	52.31%	41.98%
Overall Classification Accuracy					**45.20%**

The table shows that all classification methods overestimate the amount of agriculture and underestimate the amount of bare soil. Overall, the maximum likelihood classification proved to be the most accurate method, and therefore it was also applied to the Sunga area and used as a thematic layer for the detection of SWC measures using OBIA.

5.2 Soil and water conservation measure mapping using object-based image analysis

In figure 5.3 two typical areas with different SWC measures are depicted; an area with bench terraces and an area with grass strips. The image of the grass strips shows that these features look like regular fields with a pronounced line between them. This is due to the grass strip and an elevation drop which creates a shadow on the underlying field. This type of shadow also occurs in the fields with bench terraces but the lines are closer to one another. These shadows were used to classify the soil and water conservation measures. Because the shadows in both measures are so similar, the two were combined into single 'swc class', to increase mapping accuracy. Results of mapping of other soil and water conservation measures such as agroforestry and mulching proved to be of too low accuracy and were therefore omitted in the classification. As terraced fields can consist of both bare and cultivated areas side by side (figure 5.3), spectral information alone did not provide sufficient detail. Therefore the most important parameter for segmentation is shape, which was set to 0.6, which means that shape characteristics steered the segmentation process for 60% and spectral characteristics for 40%. This gave a higher priority for shape in the segmentation process while spectral response was still taken into account, which was necessary to distinguish between different land cover types, e.g. forest and agriculture. Bench terraces and grass strips are generally elongated features; therefore the compaction parameter was set to 0, allowing elongated objects to be formed.
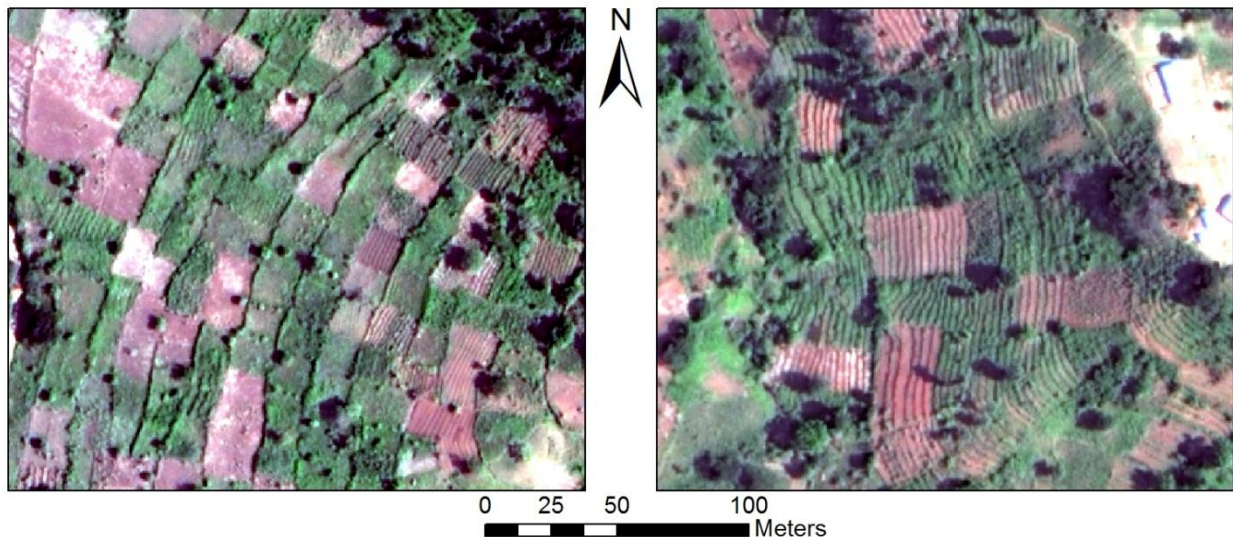
Figure 5.3: Worldview 2 image (RGB=321) of grass strips (left) and bench terraces (right) in the study area of Soni.

Three segmentation steps were taken with scale factors of 150, 10 and 7. At scale levels 10 and 7 single terrace edges or grass strips were classified. At level 10 this was done by using the density and the asymmetry of the objects as classifiers for the terrace edges, because these are elongated and are narrow and are never a perfect square at this scale level. Other objects exist with the same characteristics and need to be removed from the classification. This was done by using several other object properties. The width of the objects was an important classifier because the terrace edges are never more than 3 pixels wide. The distance to other classified edges was also used because a single terrace edge or grass strip in a single field is rare, which means that edges are in a close proximity. For scale level 7 also the mean difference in spectral response in respect to its neighbours was used as an extra object property for classification. This was done to classify the shadow which the terrace and grass strip edges create on the underlying field.

At scale level 150 the area of the objects that contained terrace edges and/or grass strips was calculated. When an object consisted for at least 5% (scale level 10) or 3% (scale level 7) of terrace edges, it was classified as an area with SWC measures. A result of visual inspection was that fields that border SWC areas for at least 30% and consists for at least 0.5% out of terrace edges in nearly all cases should also be classified as areas containing SWC measures. Figure 5.4 shows a portion of the study area near Soni on which the classification method was applied. The total area that contains soil and water conservation measures for both blocks is depicted in table 5.2.
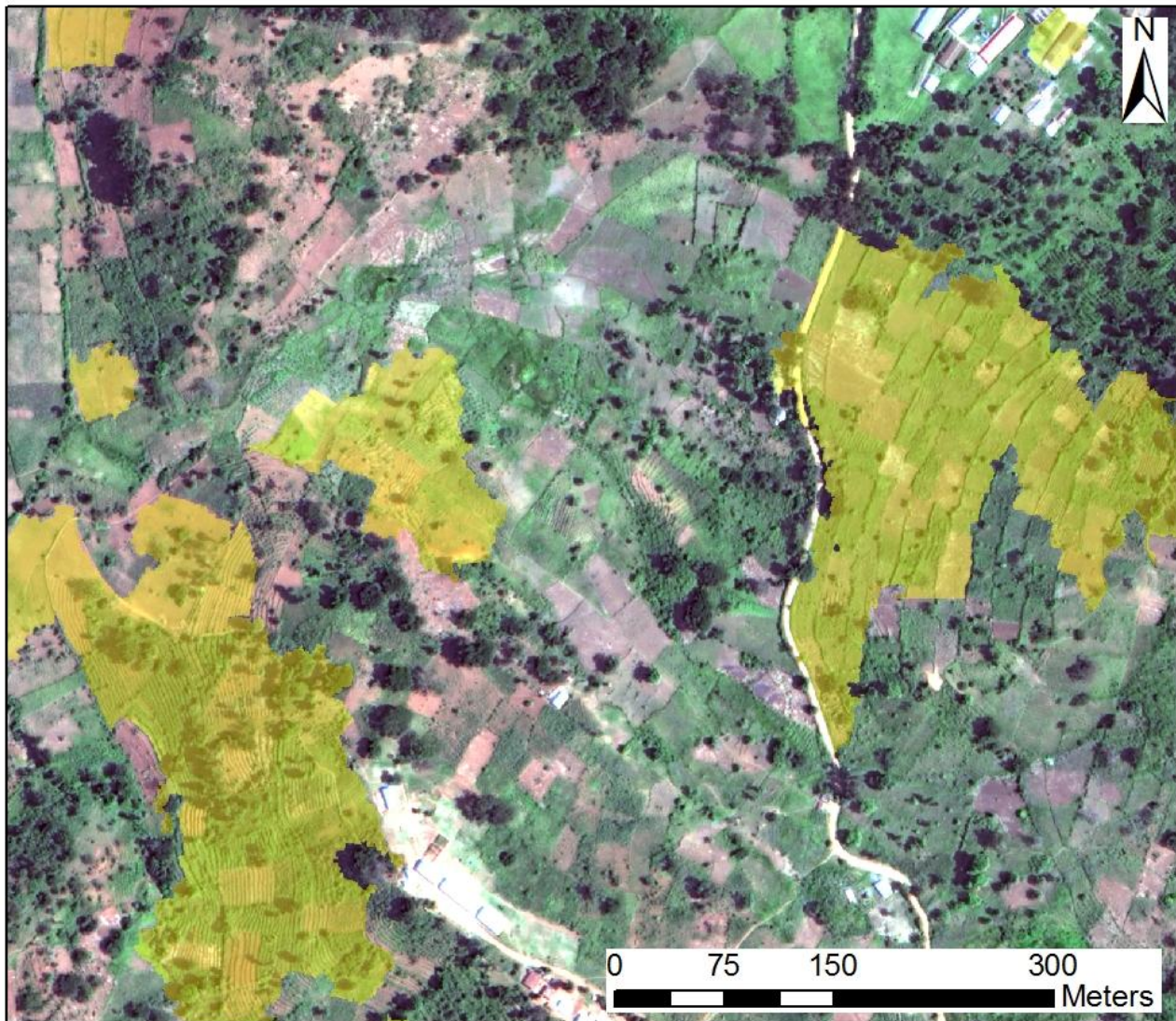
Figure 5.4: Part of the study area near Soni, where SWC measures have been classified, depicted as yellow areas.

Figure 5.4 shows a slope in the east of the figure where grass strips area present, which is almost entirely classified correctly but for a small portion at the south of the area. There are also some parts of the area with bench terraces in the west which have not been classified as being areas containing soil and water conservation measures. In the northeast of the image a house can be seen that was classified incorrectly. Table 5.2 shows that the Soni block has a larger area that is used for agriculture, while the Sunga block has the highest adoption of soil and water conservation measures.

Table 5.2 Total area classified as containing soil and water conservation measures for the Soni and Sunga blocks.

Block	Total area	Agricultural Area	Area containing SWC measures	Percentage of agricultural area containing SWC
Soni	82.5 km^2	72 km^2	2.09 km^2	2.90 %
Sunga	82 km^2	47 km^2	9.29 km^2	19.75%

Location of the SWC measures

Ranges and averages of the incline of the slopes at locations where soil and water conservation measures were classified were determined using ArcGIS. The SWC measures in the Soni area are located on slopes ranging from 0 – 35° with an average of 14.9°. For the Sunga area this range is wider; from 0- 88° with an average of 21.9°, where the extremely high values of 35° and higher are probably caused by a misclassification in the mapping of the soil and water conservation measures.

Accuracy assessment

The overall accuracy of mapping soil and water conservation measures in the two blocks ranged from 75-80% (table 5.3). Areas that have been classified as areas containing soil and water conservation measures in the image have a lower accuracy than non-SWC areas.

Table 5.3 Results of the accuracy assessment of the soil and water conservation measures for the Soni and Sunga blocks.

Soni

Classified data	Reference data			
	SWC	Non SWC	Totals	Accuracy
SWC	30	20	50	60%
Non-SWC	5	45	50	90%
Totals	35	65	100	
Overall Accuracy				75%

Sunga

Classified data	Reference data			
	SWC	Non SWC	Totals	Accuracy
SWC	34	16	50	68%
Non-SWC	6	46	50	92%
Totals	40	60	100	
Overall Accuracy				80%

5.3 Erosion risk mapping using the Universal Soil Loss Equation

The values for erosion for the mapping without soil and water conservation measures range from 0 to 100 t ha^{-1} yr^{-1} for both the Soni and Sunga areas (figure 5.5). Low values (in blue) are visible in the valley bottoms and higher values on the valley sides, especially those with a low vegetation cover. The forested areas in both maps show generally lower values than the other areas. For the Sunga map the areas where the most risk of erosion occurs is on the western and northern side of the image, where the steep slopes that descend into the plains are located. Here the high erosion values of around 100 t ha^{-1} yr^{-1} are present. Visual inspection of the images shows that the erosion values are highly related to the slope values. General values in the agricultural area range between 0- 50 t ha^{-1} yr^{-1} for the Sunga area. For the Soni area high values occur on the bedrock as this was not excluded from the mapping, while in the agricultural areas the values range between 0-100 t ha^{-1} yr^{-1}.

Locations and modelled effectiveness of the soil and water conservation measures

The modelled soil loss of the two different mapping methods (with and without SWC measures) was compared to each other. For the Soni area a total reduction of 28753.3 t for the areas with soil and water conservation measures was modelled, for the Sunga area this was 180465 t. Total average erosion values for the areas with SWC measures for both blocks are depicted in table 5.4.

Table 5.4 Total average erosion values modelled with the USLE with and without the incorporation of soil and water conservation measures, for the Soni and Sunga study areas.

	Average erosion, no SWC t/ha/yr	Average erosion, with SWC t/ha/yr	Average reduction t/ha/yr	Reduction in erosion
Soni	39.8	23.0	16.8	42.1%
Sunga	52.0	22.5	29.5	56.7%

The modelled effectiveness of the soil and water conservation measures in the Sunga area is significantly higher than the modelled effectiveness of the SWC measures in the Soni area.

Soni
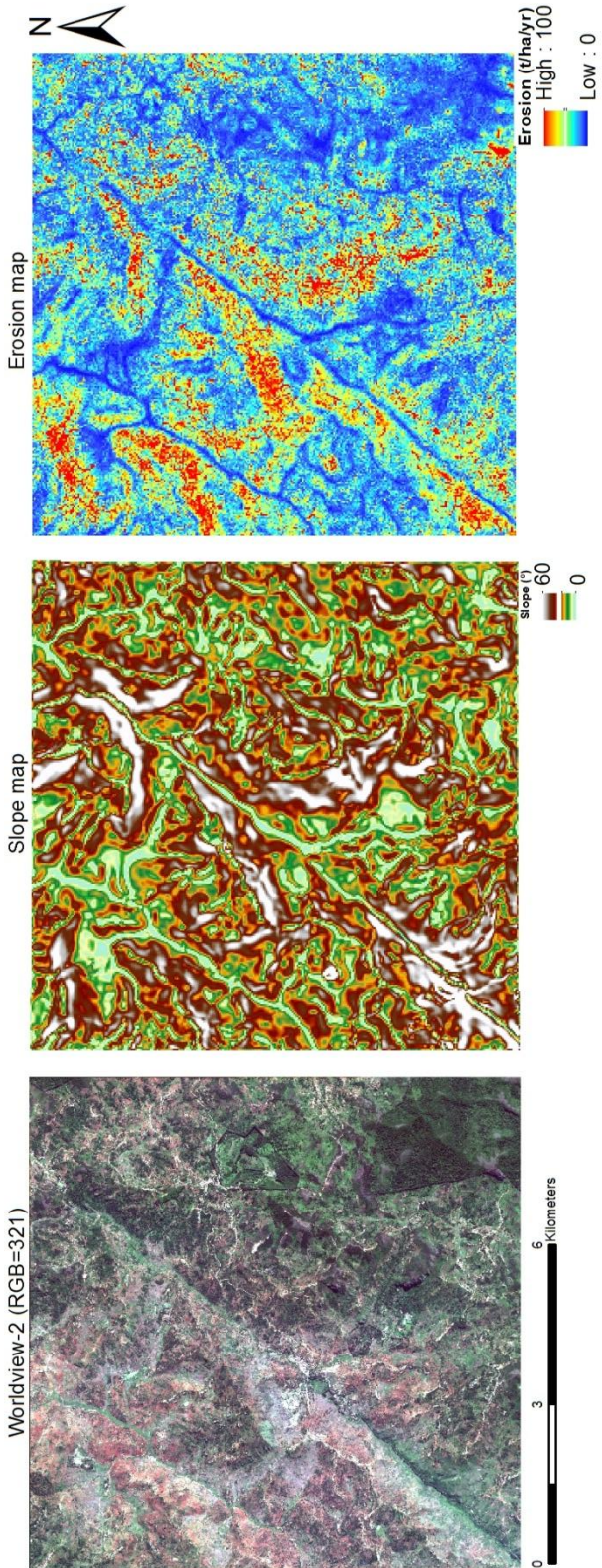
Sunga
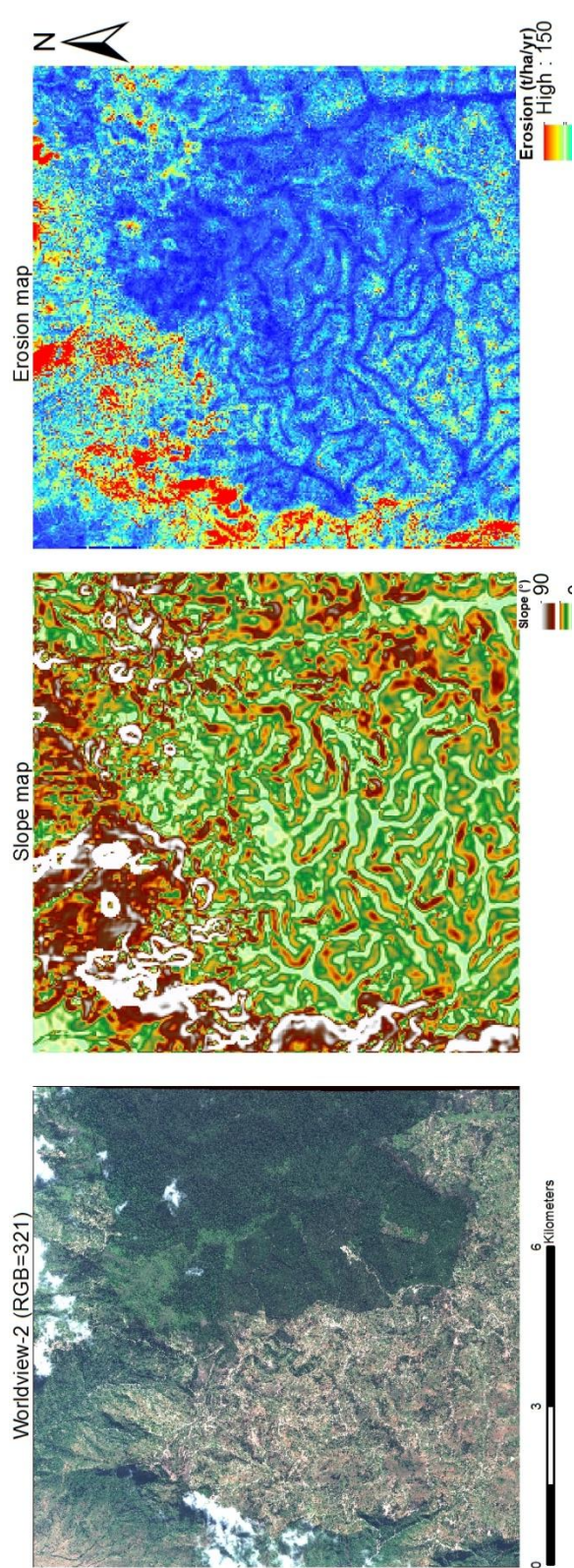
Figure 5.5 Erosion maps created with the USLE of the Soni block (top) and the Sunga block (bottom).
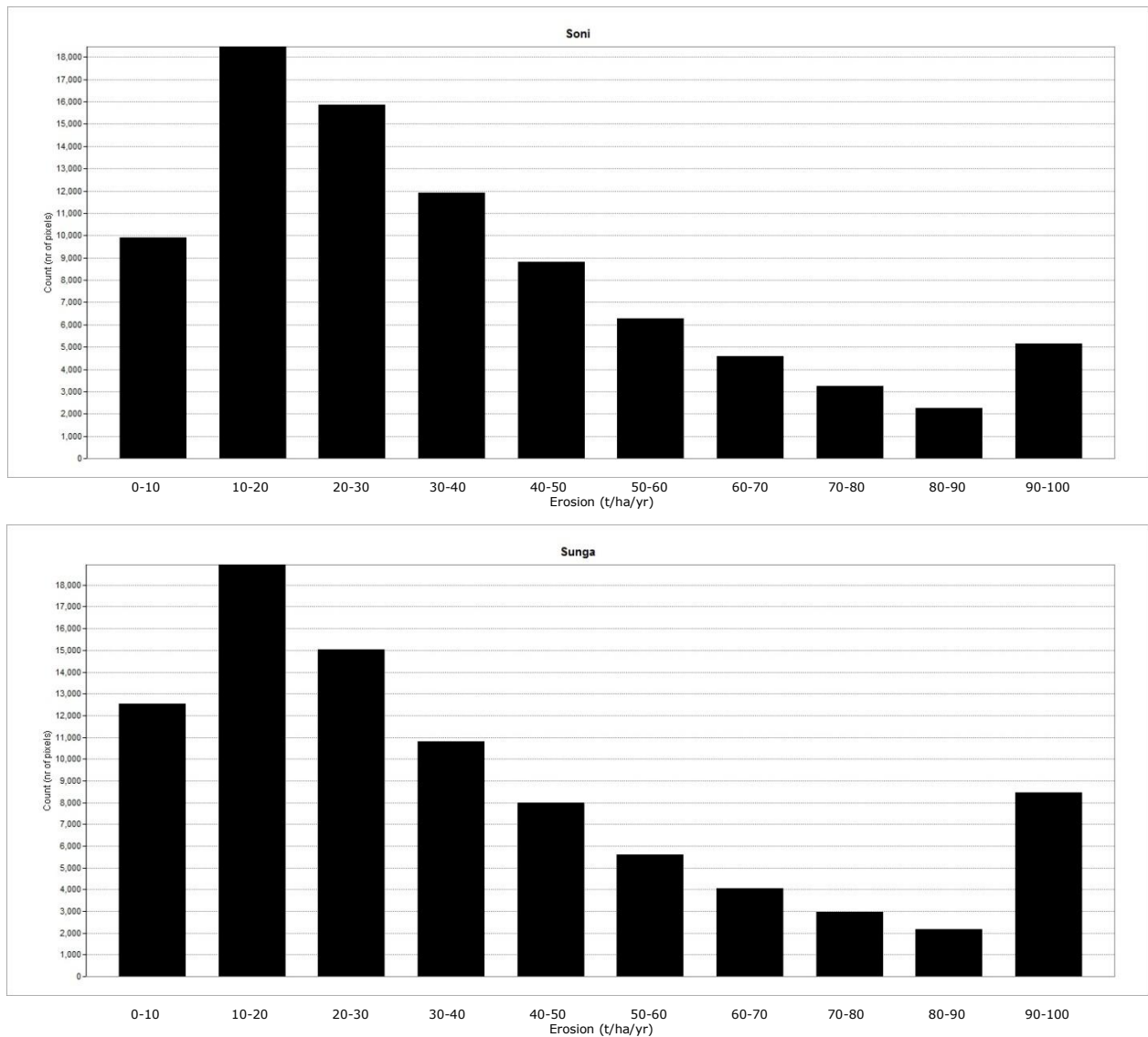
Figure 5.6: Histograms for the USLE erosion maps for the 10x10 blocks of Soni (top) and Sunga (Bottom). NB The highest classes for both areas are clumped and are therefore wider than the lower erosion classes.

Figure 5.6 shows the histograms for the erosion mapping without the use of soil and water conservation measures, using the USLE for both the Soni and the Sunga study areas. Both histograms show a similar pattern; the majority of pixels is assigned relatively low erosion, while (very) high erosion values are less numerous. The highest erosion values in the Sunga area of 100 t ha^{-1} y^{-1} are found on the edge of the mountain plateau, where slopes are very steep.

6. Discussion

6.1 Land use classification

According to the error matrix, the maximum likelihood classification method performs best with an accuracy of 51.79%. This is in contradiction with findings in many other studies where the object-based approach was more accurate (e.g. Willhauck, 2000; Yuan & Bauer, 2006). Wang et al. (2004) also found a lower accuracy for an object-based classification method (80.4%) than the maximum likelihood classification method (88.9%) for the classification of mangrove forests

When the classification methods are compared visually, the object-based method with scale level 20 seems to perform better than the maximum likelihood classification; especially the built-up areas and the shadows seem to be classified better, whereas the forested areas are classified less accurate. Reasons for the less accurate results might lie in a problem with the way of assessing the accuracy. For an object-based classification method also an object-based accuracy assessment should be used. No proper method for assessing accuracy in this way exists up to now, however. Another problem might be that objects do not represent landscape structural-functional units correctly (Hay & Castilla, 2005). This means that the objects that were created during the segmentation stage might not represent real-world landscape units.

The confusion between bare areas and built up areas, which are mainly houses with red roofs (oxidized galvanized steel plating) is difficult to solve with this type of image data because the bare areas have very similar characteristics as the roofs due to the red colour (oxidized iron) of the soils. The reflection values are similar and also shape characteristics are similar as they are both square-forms. Herold et al. (2002) also encountered this problem for an area in California, where roofs of different colours were often mixed up with bare soil. A solution for this problem could be to use satellite imagery just after a wet period, so soils have higher water content and therefore different spectral response than in a dry period. Timing of this is extremely difficult because during a wet period cloud cover is nearly always high.

In comparison to other studies which have used an object-based approach for land use mapping the accuracies that were obtained in this study are relatively low. Bock et al. (2005) found an overall accuracy of 86.2% for an area in Germany and 80.7% for an area in the United Kingdom using image data with a resolution of 20 cm and a DEM with a resolution of 1 meter. Lackner and Conway (2008) found similar accuracies of 86% and 90% for land use maps with ten and six classes respectively for an area in Ontario, Canada. Reasons for higher accuracies in those studies might include the use of a high

resolution DEM. Factors that might have had a negative impact on the classification accuracies in this study are the presence of small scale farming, the use of intercropping and agroforestry. These factors all cause high spatial heterogeneity in agricultural fields. Because the majority of the fields is rather small (100-250 m^2) many boundaries between fields (e.g. ditches, shrubs or trees) are present, which cause higher spatial heterogeneity. Reflection values between e.g. mulch and a banana tree are significantly different, but might belong to the same land use type or even field, which makes an automatic classification less accurate. Agroforestry caused classification problems in other studies as well, e.g. Lu et al. (2004), where agroforestry and coffee plantations were confused with different succession stages in natural rainforests of the Amazon in an automatic land use classification.

Over the past years, more high resolution satellite imagery has become available with the launching of e.g. Quickbird and Worldview (DigitalGlobe, Longmont, CO, USA) satellites in 2001 and 2009, respectively. These high resolution images allow for land use mapping with higher accuracies, but some negative side effects for land use mapping may occur. Where in low resolution imagery forests are homogeneous clusters of pixels, in high resolution imagery, separate shadows from single treetops can be observed. This can be a positive side effect when classifying different tree species (e.g. Quackenbush & Im, 2010) but it can negatively affect land use mapping, while spectral responses within a single forest differ, which can be seen in the classification in this study. Similarly, shadows are visible next to other high structures such as houses, which also often results in a wrong classification. The accuracy assessment shows that pixel-based classification methods have a larger problem with this; the accuracy for bedrock is low for both pixel-based methods, which is due to classifying shadows as being bedrock. These problems are partly solvable with the object-based image analysis method but not for the pixel-based methods. The solution for the object-based methods is not ideal either due to a limited distinction between shadows.

The timing of the fieldwork and the date of the Worldview-2 image was not similar. As there was no precipitation data available for the period preceding the date of the Worldview-2 image, it is not completely clear what the differences between e.g. the vegetation cover were. Local sources claim that there was significantly more precipitation in the 'short rains' of 2009 than in 2010, which means that vegetation cover was higher on the image than during the fieldwork campaign. This might have led to errors in the accuracy assessment due to changed land cover.

6.2 Soil and water conservation measure mapping

Up to now, no other studies have tried to locate soil and water conservation measures in an agricultural area by ways of automatic detection in remote sensing imagery. Other features in the landscape however have been successfully located with similar high accuracy results (e.g. Addink & Kleinhans 2008).

The size of the SWC measures is an important factor in their classification on the basis of remotely sensed images. With diminishing size of the measures, the accuracy diminishes. When terrace edges (shadows) become smaller than about 0.5 meter, which is about the resolution of the panchromatic band in the WV-2 image, they are no longer classified as terraces. Therefore when classifying these kinds of SWC measures an H-resolution model (Woodcock and Strahler, 1986) is needed. This means that the objects to be classified were larger than a single image pixel.

Problems with misclassifications of SWC measures arise in built up areas that have not been distinguished as being built-up in the land use mapping and therefore have not been masked out in the classification process. As houses also form elongated objects with very similar characteristics as bare, terraced fields, some built-up areas are misclassified as being an area with SWC measures. Better results would have been obtained when a land use map with higher classification accuracies would have been available. A land use map with a classification accuracy of 80% or preferably higher would be advisable.

The SWC classifications need to be improved to be able to say more about the total area containing SWC measures. There are several ways to improve this accuracy: a better land use map will cause less confusion between houses and SWC measures. In the case of a 100% accurate classification of built-up areas, no houses would have been classified as soil and water conservation measures. The accuracy of the proposed method of classifying the SWC measures with aid of the inclination and aspect of a slope could improve the classification accuracy drastically if a high resolution DEM would have been available. For this purpose a DEM with a horizontal resolution of approximately 5 meter would be necessary.

The position of the sun is an important factor when classifying soil and water conservation measures. The position of the sun can either cast small, large or no shadows at all of i.e. bench terraces. Figure 6.1 depicts similar bench terraces on two sides of a valley. In this figure the terraces on the west side of the valley are less clear due to the absence of shadows.

Figure 6.1: Similar bench terraces on two sides of a valley running from north to south in the Sunga study area. The terraces in the east are more clearly visible due to the shadows of the terraces. NB: The sun is positioned in the east.

Tenge (2005) reported that grass strips and bench terraces should ideally be placed on slopes with an incline of 22-40%. The average slope values where the SWC measures are located in the study areas were 26.6% for the Soni area and 40.2% for the Sunga area, which correspond to the ideal values found by Tenge (2005). The lower (0°) and higher (88°) boundaries of slope values where SWC measures were classified are mostly wrongly classified areas, which was determined visually. Especially areas with an extremely steep slope where SWC measures were classified in the Sunga area were classified wrongly as they are positioned on the steep ridges that are at the edge of the mountain plateau, where no form of agriculture is possible.

6.3 Erosion risk mapping with the Universal Soil Loss Equation

The modelled erosion values that range from 0 to 100 t ha^{-1} yr^{-1} for both the Soni and Sunga are high, and would have been even higher if not for the set threshold of 100 t ha^{-1} yr^{-1}. Values in literature give an indication of erosion in the Usambara Mountains of up to 100 t ha^{-1} yr^{-1} (Pfeiffer, 1990; Shelukindo & Kilasi, 1993; Kaswamila, 1995; Lyamchai et al., 1998). Some other modelling studies that have used the USLE also found high erosion values; 362 t ha^{-1} yr^{-1} for an area in Turkey (Gitas et al., 2009) and 155.53 t ha^{-1} yr^{-1} for an area in India (Dabral et al., 2008). The main reason for these high values to occur is the presence of steep slopes. The USLE is not suitable for slopes that are steeper than 20% (Wischmeier & Smith, 1974).

When looking at the histogram for the Sunga area, the majority of the pixel values are relatively low; up to 50 t ha^{-1} yr^{-1} for the agricultural areas, which correspond to the other reported values of up to 100 t ha^{-1} yr^{-1}. Values for the Soni agricultural area however, seem extremely high, with modelled erosion values reaching up to approximately 200 t ha^{-1} yr^{-1}. The reason for this difference between the two blocks lies partly in a higher R factor for the Soni area. The R factor for the Soni area was 275.16, while the R factor for the Sunga area was 218.46. This means that all erosion values become 1.26 times higher for the Soni area than for the Sunga area. This is however not the only explanation, as erosion values for the Soni area are up to four times as high as the values for the Sunga area. The other reason is an overestimation of the LS parameter, which is a common problem when modelling soil erosion using slopes extracted from a DEM (Hickey, 2000).

The most important parameter for assessing the quantitative erosion with the USLE in this case was the LS factor, for this factor had the largest range (table 7.1). Because the USLE was developed for gentle to medium slopes the ranges in the areas with steep slopes far exceed LS values that are generally used in the USLE (Wischmeier & Smith, 1978).

Table 6.1 Ranges (min-max) of the parameters of the USLE for the Soni and Sunga study areas.

Location	R	K	LS	C	P
Soni	NA	0.016-0.069	0-57.28	0-1	0.5-1
Sunga	NA	0.032-0.057	0-115.37	0-1	0.5-1

From table 6.1 can be seen that the range for the LS parameter in the Sunga is the largest and therefore has the highest erosion values. These values only occur on the steep slopes at the edge of the mountain plateau. This is also clearly visible when comparing the slope map and the USLE erosion map (figure 5.5). The LS values in the agricultural area of Soni are significantly higher than those in the Sunga area. In the areas containing soil and water conservation measures the LS values are lower for the Soni area, which could be due to a misclassification of SWC measures in the Sunga areas with steep slopes, like on the edges of the mountain plateau.

Tenge (2005) reported that the effectiveness of different soil and water conservation measures in the Usambara Mountains ranged from 96-99% for soil loss. The USLE modelled an effectiveness of the SWC measures of 42-57%, which is significantly lower than the measured values by Tenge (2005). This could be calibrated by changing the

support practice factor P and the slope and slope length factor LS accordingly. The reason for the lower modelled effectiveness in the Soni area compared to the Sunga area lies within the slope and slope length factor, as the P factor changes equally for both areas.

Parameters for the model have been generalised as measuring the exact parameters for the USLE for an area of 80 km^2 would be too laborious, if not impossible to do. This generalisation applies to all of the 5 parameters in the equation. Some parameters however might be more affected by this generalisation than others. Especially the LS, C and P factors were heavily generalised. For the LS factor this means that values range to either a high or low extreme, which is partly due to the generalisation of the values for slope length in terraced areas. Normally different types of terraces and grass strips produce a different slope length, where here it is all generalised. The same can be said for the support practice factor P where all areas with SWC measures have been given a value of 0.5. C values are only calculated using the image derived NDVI, which means that features as rock cover and residue mulch are not accounted for. The rainfall factor R has also been generalised due to a lack of rainfall data.

7. Conclusions and recommendations

This study used several remote sensing and field methods to locate soil and water conservation measures and model their effectiveness in the Lushoto district in the West Usambara Mountains, Tanzania.

At a smaller scale land use maps were created using four different classification methods on Worldview-2 images; a (1) minimum distance to means, (2) a maximum likelihood, (3) an Object-based with scale level 50 and (4) an object-based with scale level 20 classification method, of which the maximum likelihood classifier proved to be the most accurate with an accuracy of 52%. However, classes of interest, i.e. agricultural areas and bare areas have user's accuracies of up to 100%. The low accuracy values are probably a result of a highly dissected topography combined with the presence of small scale farming and the use of intercropping.

The land use map created with the maximum likelihood classification method was used to create soil and water conservation (SWC) measures maps, on which SWC measures were either bench terraces or grass strips. These maps were created using object-based image analysis, with an eventual accuracy of 75-80%. The total area containing soil and water conservation measures was 2.09 km^2 for the Soni area which represents approximately 3% of the entire agricultural area and 9.29 km^2 for the Sunga area which represents approximately 20% of the entire agricultural area. These values are an overestimation due to misclassification of e.g. buildings.

In order to achieve higher accuracies for the mapping of soil and water conservation measures in future studies a high resolution digital elevation model and a land use map with a higher accuracy need to be used. The digital elevation model could be used to relate the direction of the valleys to the direction of the soil and water conservation measures and to mask out areas which are flat or too steep for soil and water conservation measures. A more accurate land use map would result in less misclassification of e.g. buildings.

A quantitative erosion risk mapping was performed on the Worldview-2 images with the Universal Soil Loss Equation (USLE). The map with the locations of the soil and water conservation measures served as an input for the slope and slope length factor and the support practice factor of the USLE. The map showed similar patterns as the larger erosion risk map, mainly following slope and cover values. Modelled erosion values ranged from 0-50 t ha^{-1} yr^{-1} in the agricultural area of Sunga and 0-200 t ha^{-1} yr^{-1} in the

Soni area. This probable overestimation of erosion in the Soni area is mainly due to an overestimation of the slope and slope length factor LS.

The modelled effectiveness of the soil and water conservation measures was 42-58%, which is significantly lower than reported literature values for the same area and conservation measures. To model this effectiveness more accurately a calibration of the slope and slope length factor and the support practice factor in the Universal Soil Loss Equation is necessary, because these factors are (partly) dependent on the existence of soil and water conservation measures.

This study showed that it is possible to distinguish relatively small SWC measures in satellite imagery, provided that the pixel size of the imagery is smaller than the width of the measures, which generally is 1-2 m. It is possible to distinguish SWC measures, as long as an H-resolution model is present. Results can be improved by using a higher resolution DEM and a land use map with a higher accuracy, which in turn is difficult to acquire in this type of environments due to high spatial heterogeneity.

In summary, future studies that are aimed at the automatic classification of soil and water conservation measures or other features in a landscape with a high spatial heterogeneity using object-based image analysis should take the following into account:

-Thematic layers e.g. a land use map or digital elevation model should be of high accuracy (overall accuracy>80%) to ensure a correct classification of the features that need to be classified.
-The spatial resolution of the used imagery needs to be sufficiently high, i.e. the pixel size of the imagery needs to be significantly smaller than the features that are to be classified.
-Timing of satellite imagery and ground-truth data need to be overlapping to obtain meaningful classification accuracy assessments.

References

Addink, E.A., Kleinhans, M.G., 2008. Recognizing meanders to reconstruct river dynamics of the Ganges. GEOBIA (Pixels, Objects, Intelligence: Geographic Object-based Image Analysis for the 21st Century), Calgary, Canada 6-7 August

AHI (African Highland Initiative). 2000. Lushoto benchmark site, Annual Report. Lushoto, Tanzania. In: Tenge, A.J.M., 2005. Participatory appraisal for farm-level soil and water conservation planning in west Usambara highlands, Tanzania. Tropical Resource Management Papers 63.

ArcGIS 10 Desktop help, Redlands, California, USA. http://help.arcgis.com/en/arcgisdesktop/10.0/help/index.html

Benz, U.C., Hofmann, P., Willhauck, G., Lingenfelder, I., Heynen, M., 2004. Multiresolution, object-oriented fuzzy analysis of remote sensing data for GIS-ready information. ISPRS Journal of Photogrammetry and Remote Sensing 58 (3-4), pp. 239-258.

Bewket, W. 2002. Land Cover Dynamics Since the 1950s in the Chemoga Watershed, Blue Nile Basin, Ethiopia. Mountain Research and Development; 22 (3), 2002), pp. 263-269.

Blaschke, T., Strobl, J., 2001. What's wrong with pixels? Some recent developments interfacing remote sensing and GIS. GIS, Zeitschrift für Geoinformationssysteme 14 (6), pp. 12-17.

Blaschke, T., 2010. Object-based image analysis for remote sensing. Journal of Photogrammetry and Remote Sensing 65, pp. 2-16.

Blaszczynski, J., 1992. Soil loss prediction utilizing the RUSLE/GIS interface. Geographic Information systems and mapping-Practices and Standards, ASTM STP 1126, Johnson, A.I., Petterson, C.B., Fulton, J.L (Eds), American Society for Testing and Materials, Philadelphia, 1992, pp. 122-131.

Bocco, G., 1991. Gully erosion: processes and models. Progress in Physical Geography 15 (4), pp.392-406. Bock, M., Xofis, P., Mitchley, J., Rossner, G., Wissen, M., 2005. Object-oriented methods for habitat mapping at multiple scales – Case studies from Northern Germany and Wye Downs, UK. Journal for Nature Conservation 13 (2-3), pp. 75-89.

Casenave, A., Valentin, C., 1989. Les états de surface de la zone sehélienne. Influence sur l'infiltration. ORSTOM, Paris. In: Barthès, B., Azontonde, A., Boli, B.Z., Prat, C., Roose, E., 2000. Field- scale run-off and erosion in relation to topsoil aggregate stability in three tropical regions (Benin, Cameroon, Mexico). European Journal of Soil Science 51, pp. 485,495.

Chander, G., B. Markham, and D. Helder, 2009. Summary of current radiometric calibration coefficients for Landsat MSS, TM, ETM+, and EO-1 ALI sensors. Remote Sensing of the Environment, Vol. 113, pp. 893-903.

Dabral, P.P., Baithuri, N., Pandey, A., Soil Erosion Assessment in a Hilly Catchment of North Eastern India Using USLE, GIS and Remote Sensing. Water Resource Management 22, pp. 1783-1798.

Darwish, A., Leukert, K., Reinhardt, W., 2003. Image segmentation for the purpose of object-based classification. In: Geoscience and Remote Sensing Symposium, 2003. IGARSS '03. 2003 IEEE International (3), pp. 2039-2041. In: Blaschke, T., 2010. Object based image analysis for remote sensing. Journal of Photogrammetry and Remote Sensing 65, pp. 2-16.

De Jong, S.M., 1994. Derivation of vegetative variables from a Landsat TM image for modelling soil erosion. Earth Surface Processes and Landforms 19, pp. 165-178.

De Roo, A.P.J., Wesseling, C.G., Cremers, N.H.D.T., Offermans, R.J.E., Ritsema, C.J., Van Oostindie, K., 1994, LISEM: a new physically-based hydrological and soil erosion model in a GIS-environment, theory and implementation. IAHS publication 224, pp. 439-448.

De Roo, A.P.J., Wesseling C.G, Ritsema, C.J., 1996a, LISEM: a single-event physically based hydrological and soil erosion model for drainage basins. I: Theory, input and output. Hydrological Processes 10, pp. 1107-1117.

De Roo, A.P.J., Offermans. R.J.E., Cremers, N.H.D.T., 1996b, LISEM: a single-event, physically based hydrological and soil erosion model for drainage basins. II: Sensitivity analysis, validation and application. Hydrological Processes 10, pp. 1119-1126

eCognition Developer 8.64.0 Reference book, document version 8.64.0, 2010. Trimble Germany GmbH, Trappentreustr. 1, D-80339 München, Germany. http://www.ecognition.com/

Eswaran, H., Lal, R., Reich, P.F., 2001. Land degradation: an overview. In: Bridges, E.M, Hannam, I.D., Oldeman, L.R., Penning de Vries, F.W.T., Scherr, S.J., Sombatpanit S. Response to land degradation. Science Publishers Inc., Enfield, NH, USA, pp. 20-35.

FAO: 1998. Food Balance Sheet. In: Pimentel, D., 2005. Soil erosion: A food and environmental threat. Environment, Development and Sustainability 8, pp. 119-137. Geological Survey Tanzania, 1965. Geological map, 1:250.000, Quarter degree sheet 91 and 110. Daluni.

Feoli, E., Vuerich, L.G., Zerihun, W., 2002. Evaluation of environmental degradation in northern Ethiopia using GIS to integrate vegetation, geomorphological, erosion and socio- economic factors. Agriculture, Ecosystems and Environment 91 (1-3), pp. 313-325.

Fisher, P, Comber, A.J., Wadsworth, R., 2005. Land use and land cover: Contradiction or Complement. In: Fisher, P., Unwin, D., 2005. Re-Presenting GIS. Chichester: Wiley. pp. 85–98.

Flanders, D., Hall-Beyer, M., Pereverzoff, J., 2003. Preliminary evaluation of eCognition object-based software for cut block delineation and feature extraction. Canadian

Journal of Remote Sensing 29 (4), pp. 441-452.

Gitas, I.Z., Douros, K., Minakou, C., Sileos, G.N., Karydas, C.G., 2009. Multi-temporal soil erosion risk assessment in N. Chalkdiki using a modified USLE raster model. EARSel eProceedings 8, 2009, pp. 40-52.

Hay, G.J., Catilla, G., 2005. Object-based image analysis: Strengths, weaknesses, opportunities and threats (SWOT). OBIA, 2006: The international archives of the photogrammetry, remote sensing and spatial information sciences, Salzburg, Austria..

Hay, G.J., Castilla, G., 2008. Geographic Object-Based Image Analysis (GEOBIA): A new name for a new discipline. In: Blaschke, T., Lang, S., Hay, G. (Eds.), Object-based Image Analysis. Springer, Heidelberg, Berlin, New York, pp. 93_112.

He, H.S., Mladenoff, D.J., Radeloff, V.C., Crow, T.R., 1998. Integration of GIS data and classified satellite imagery for regional forest assessment. Ecological Applications 8 (4), pp. 1072-1083.

Heijnen, J.D., 1974. National policy, foreign aid and rural development. A case study of LIDEP's vegetable component in Lushoto District (Tanzania). Department of Geography of developing countries, Geogr. Inst., Universiteit Utrecht. 165 pp. In: Holben, B., Justice, C., 1981. An examination of spectral band ratioing to reduce the topographic effect on remotely sensed data. International Journal of Remote Sensing 2 (2), pp. 115-133.

Hénin, S., Monnier, G., Combeau, A., 1958. Méthode pour l'étude de la stabilité structural des sols. Annales Agronomiques 9, pp. 73-92. In: Barthès, B., Azontonde, A., Boli, B.Z., Prat, C., Roose, E., 2000. Field- scale run-off and erosion in relation to topsoil aggregate stability in three tropical regions (Benin, Cameroon, Mexico). European Journal of Soil Science 51, pp. 485,495.

Herold, M., Scepan, J., Muller, A., Gunther, S., 2002. Object-oriented mapping and analysis of urban land use/cover using IKONOS data. Proceedings of 22nd EARSEL Symposium "Geoinformation for European-wide integration, Prague, June 2002.

Hessel, R., Messing, I., Liding, C., Ritsema, C. and Stolte, J., 2003. Soil erosion simulations of land use scenarios for a small Loess Plateau catchment. Catena 54(1-2), pp. 289-302.

Hickey, R., 2000, Slope Angle and Slope Length Solutions for GIS. Cartography 29 (1), pp. 1 - 8.

Jürgens, C., Fander, M., 1993. Soil erosion assessment and simulation by means of SGEOS and ancillary data. International Journal of Remote Sensing 14 (15), pp. 2847-2855.

Kaswamila, A.L., 1995. Assessment of the effectiveness of certain soil conservation practices by soil surface microtopographic features. A case study of Mlesa, Mwangoi in the West Usambara mountains (Tanzania). M. Sc. Thesis. ITC, Enschede, The Netherlands. In: Tenge, A.J.M., 2005. Participatory appraisal for farm-level soil and

water Conservation planning in west Usambara highlands, Tanzania. Tropical Resource Management Papers 63.

Kirkby, M.J., Abrahart, R., McMahon, M.D., Shao, J., Thornes, J.B., 1998. MEDALUS soil erosion models for global change. Geomorphology 24 (1), pp. 35-49.

Laben, C.A., Brower, B.V., 2000. Process for Enhancing the Spatial Resolution of Multispectral Imagery Using Pan-Sharpening, US Patent 6,011,875.

Lackner, M., Conway, T.M., 2008. Determining land-use information from land cover through an object-oriented classification of IKONOS imagery. Canadian Journal of Remote Sensing 34 (2), pp. 77_92.

Lal, R., 1988, Soil degradation and the future of agriculture in sub-Saharan Africa. Journal of Soil and Water Conservation 46 (6), pp. 444-451.

Lal, R., Stewart, B.A., 1990. Soil degradation, New York, Springer-Verlag. In: Pimentel, D., 2005. Soil erosion: A food and environmental threat. Environment, Development and Sustainability 8, pp. 119-137.

Lal, R., Elliot, W., 1994. Erodibility and erosivity. Soil Erosion: Research Methods, edited by R Lal. Soil and Water Conservation Society (St. Lucie Press, Florida, USA), pp.181-208.

Lal, R., 1995. Erosion-Crop Productivity Relationship for the soils of Africa. Soil Science Journal 59, pp. 661-667.

Lal, R., 2001. Soil degradation by erosion. Land degradation and Development 12, pp. 519- 539.

Lane, L.J., Nearing, M.A., 1989. USDA—Water Erosion Prediction Project: profile model documentation. NSERL Report No 2, USDA–ARS National Soil Laboratory, W. Lafayette, Ind. In: Kirkby, M.J., Abrahart, R., McMahon, M.D., Shao, J., Thornes, J.B., 1998. MEDALUS soil erosion models for global change. Geomorphology 24 (1), pp. 35-49.

Le Bissonnais, Y., 1996. Aggregate stability and assessment of soil crustability and erodibility: I. Theory and methodology. European Journal of Soil Science 47, pp. 425-437.

Liversage, V., 1944. Rural reconstruction in East Africa. East Africa Forestry Journal 10, pp.120-124.

Lo, A., El-Swaify, S.A., Dangler, E.W., Shinshiro, L., 1985. Effectiveness of El30 as an erosivity index in Hawaii. In: S.A. E1-Swaify, W.C. Moldenhauer and A. Lo (Editors),

Lyamchai, C., Owenya, M., Ndakidemi, O., Massawe, N., 1998. Participatory Rural Appraisal in Kwalei catchment Lushoto, Tanzania. In: Lyimo SD, Ndondi RV (Eds). Selian Agricultural Research Institute, Arusha. In: Tenge, A.J.M., 2005. Participatory appraisal for farm-level soil and water conservation planning in west Usambara highlands, Tanzania.

Tropical Resource Management Papers 63. Soil Erosion and Conservation. In: Renard,

K.G., Freimund, J.R., 1992. Using monthly precipitation data to estimate the R-factor in the revised USLE, Journal of Hydrology 157, pp. 287-306. Soil Conservation Society of America, Ankeny, pp. 384-392.

Lu, D., Mausel, P., Batistella, M, Moran, E., 2004. Comparison of Land-Cover classification methods in the Brazillian Amazon Basin. Photogrammetric Engineering & Remote Sensing70 (6), pp. 723-731.

Lubczynski, M.W., Gurwin, J., 2005. Integration of various data sources for transient groundwater modelling with spatio-temporally variable fluxes-Sardon study case, Spain.Journal of Hydrology 306(1-4), pp. 71-96.

Lundgren, L., 1978. Soil Conditions and Nutrient Cycling under natural and plantation forests in Tanzanian Highlands. Reports in Forest Ecology and Forest Soils 31, Department of forest soils, Swedish University of Agricultural Sciences, Uppsala, 426 pp.

Lundgren, L., 1980. Comparison of surface runoff and soil loss from runoff plots in forest and small-scale agriculture in the Usambara Mts, Tanzania. Geografiska Annaler. Series A, Physical Geography 62 (3/4), pp. 113- 148.

Mati, B.M., Morgan, R.P.C., Gichuki, F.N., Quinton, J.N., Brewer, T.R., Liniger, H.P., 2000. Assessment of erosion hazard with the USLE and GIS: A case study of the Upper Ewaso Ng'iro North basin of Kenya. International Journal of applied Earth Observation and Geoinformation 2 (2), pp. 78-86.

McBratney, A.B., Santos, M.L.M., Minasny, B., 2003. On digital soil mapping. Geoderma 117 (1-2), pp. 3-52.

Moore, I.D., Turner, A.K., Wilson, J.P., Jenson, S.K., Band, L.E., 1993. GIS and land-surface-subsurface process modeling. Environmental Modeling with GIS, edited by Goodchild, M.F., Parks, B.O., Steyaert, L.T., (Oxford University Press, U.K.) pp. 196-230.

Morgan, R.P.C., Morgan, D.D.V., Finney, H.J.,1984. A predictive model for the assessment of erosion risk. J. Agricultural Engineering Research 30. pp.245- 253.

Mowo, J., Mwihomeke, S., Mzoo, J. and Msangi T. 2002. Managing natural resources in the West Usambara mountains: A glimmer of hope in the horizon. Ministry of Agriculture and Food Security, Tanzania.
http://www.mtnforum.org/resources/library/mowo02a.htm

Pfeiffer, R., 1990. Sustainable Agricultural in practice- The production potential and environmental effects of macro-contour lines in west Usambara Mountains, Tanzania.Ph.D. dissertation. Hohenheim University, Germany. In: Tenge, A.J.M., 2005. Participatory appraisal for farm-level soil and water conservation planning in west Usambara highlands, Tanzania. Tropical Resource Management Papers 63.

Pimentel, D., 1993. World Soil Erosion and Conservation, Cambridge, UK, Cambridge University Press. . In: Pimentel, D., 2005. Soil erosion: A food and environmental

threat. Environment, Development and Sustainability 8, pp. 119-137.

Pimentel, D., Harvey, C., Resosudarmo, P., Sinclair, K., Kurz, D., McNair, M., Crist, S., Shpritz, L., Fitton, L., Saffouri, R., Blair, R., 1995. Environmental and economic costs of soil erosion and conservation benefits. Science 267, pp. 1117-1123.

Pimentel, D., Kounang, N., 1998. Ecology of soil erosion in ecosystems. Ecosystems 1, pp. 416-426.

Pimentel, D., 2005. Soil erosion: A food and environmental threat. Environment, Development and Sustainability 8, pp. 119-137.

Renard, K.G., Freimund, J.R., 1992. Using monthly precipitation data to estimate the R-factor in the revised USLE, Journal of Hydrology 157, pp. 287-306.

Roose, E., 1996. Land Husbandry: Components and Strategy. FAO Soils Bulletin 70, FAO, Rome.

Sanchez, P.A., 1976. Properties and management of soils in the tropics. Wiley & Sons, New York, USA, 618p. In: Lundgren, L., 1978. Soil Conditions and Nutrient Cycling under natural and plantation forests in Tanzanian Highlands. Reports in Forest Ecology and Forest Soils 31, Department of forest soils, Swedish University of Agricultural Sciences, Uppsala, 426 pp.

Semgalawe, Z.M., 1998. Household Adoption Behaviour and Agriculture Sustainability in the northern mountains of Tanzania. The case of Soil Conservation in the North Pare and West Usambara Mountains. Ph.D. Thesis. Wageningen Agricultural University. In:Tenge, A.J.M., 2005. Participatory appraisal for farm-level soil and water Conservation planning in west Usambara highlands, Tanzania. Tropical Resource Management Papers 63.

Shelikundo, H., Kilasi, G., 1993. Development experience and re-orientation of soil erosion control and agroforestry activities in west Usambara mountains, Tanzania. A paper presented at the workshop on Natural agroforestry and environment, SUA, Morogoro, Tanzania. In: Tenge, A.J.M., 2005. Participatory appraisal for farm-level soil and water conservation planning in west Usambara highlands, Tanzania. Tropical Resource Management Papers 63.

Shelukindo, H., 1995. Technical recommendations for soil and water conservation measures and agroforestry systems jointly developed by SECAP and TIP. Biological and physical soil and water conservation measures. Daldo, Lushoto, Tanzania. In: Tenge, A.J.M., 2005. Participatory appraisal for farm-level soil and water conservation planning in west Usambara highlands, Tanzania. Tropical Resource Management Papers 63.

Sonneveld, B.G.J.S., 2003. Measurement of erosion: is it possible? In: Gabriels, D., Cornelis, W., (Editors), Proceedings of the International Symposium on 25 years of Assessment of Erosion. Ghent University, Ghent, Belgium, pp. 53-59

Strahler, A.H., 1986. On the Nature of Models in Remote Sensing. Remote sensing of

environment 20, pp.121-139.

Šúri, M., Cebecauer, T., Hofierka, J., Fulajtár jun., E., 2002. Soil Erosion Assessment of Slovakia at a Regional Scale Using GIS. Ecology (Bratislava) 21 (4), pp. 404-422.

Tenge, A.J., 2005. Participatory appraisal for farm-level soil and water conservation planning in West Usambara highlands, Tanzania. Tropical resource management papers 63. ISBN 90-6754-904-5

Toutin T., Cheng, P., 2003. Comparison of automated digital elevation model extraction results using along-track ASTER and across-track SPOT stereo images. Optical Engineering 41 (9), pp. 2102-2106.

Van der Werff, H.M.A., van der Meer, F.D., 2008. Shape-based classification of spectrally identical objects. ISPRS Journal of Photogrammetry and Remote Sensing 63 (2), pp. 251- 258.

Vrieling, A., Sterk, G., Vigiak, O., 2006. Spatial evaluation of soil erosion risk in the west Usambara Mountains, Tanzania.Land Degradation and Development 17, pp. 301- 319.

Vrieling, A., Rodrigues, S.C., Bartholomeus, H., Sterk, G., 2007. Automatic identification of erosion gullies with aster imagery in the Brazilian Cerrados. International Journal of Remote Sensing 28(12), pp. 2723-2738.

Welch, R. and W. Ahlers, 1987. "Merging Multiresolution SPOT HRV and Landsat TM Data." Photogrammetric Engineering & Remote Sensing, 53 (3), pp. 301-303.

Wickama, J., 2010. Influence of biophysical aspects on the performance of sustainable land management measures in the Usambara Highlands of Tanzania, research proposal, Wageningen University.

Willhauck G., 2000. Comparison of object-oriented classification techniques and standard image analysis for the use of change detection between SPOT multispectral satellite images and aerial photos. In: Proceedings, ISPRS, Vol. XXXIII.

Wischmeier, W. H., Smith, D.D., 1978. Predicting rainfall erosion losses-a guide to conservation planning. US Department of Agriculture Handbook No. 537.

Woodcock, A.H., Woodcock, C.E., Smith, J.A., 1986. On the Nature of Models in Remote Sensing. Remote Sensing of Environment 20, pp. 121-139.

Yoder, R.E., 1936. A direct method of aggregate analysis of soils and a study of the physical nature of erosion losses. Journal of the American Society of Agronomy, 28, pp. 337-351. In: Barthès, B., Azontonde, A., Boli, B.Z., Prat, C., Roose, E., 2000. Field-scale run-off and erosion in relation to topsoil aggregate stability in three tropical regions (Benin, Cameroon, Mexico). European Journal of Soil Science 51, pp. 485,495.

Yuan, F., Bauer, E.M., 2006. Mapping impervious surface área using high resolution imagery: a comparison of object-based and per pixel classification. ASPRS Annual Conference 2006, Reno, Nevada, USA.

Appendix

Appendix I: Erosion Risk Map of the entire Lushoto district

An Erosion Risk Map (ERM) was created using the method proposed by Vrieling et al. (2006), which entails creating the ERM from a slope map and a fractional vegetation cover (FVC) map, using a decision tree. Vrieling et al.(2006) found that a significant (R^2=0.80) relationship exists between the Normalised Difference Vegetation Index (NDVI) and the fractional vegetation cover for a 70 km^2 large study area in the Usambara mountains, Tanzania ($R^2 = 0.80$).

In order to obtain the NDVI map from the Landsat ETM+ image, first the digital numbers of the image bands 3 and 4 were converted into reflectance values using ENVI software (version 4.7, ITT, Boulder, CO, USA), which uses a calibration method proposed by Chander et al. (2009). Subsequently the NDVI was calculated from the reflectance values using equation 1.

The relation between FVC and the NDVI that Vrieling et al. (2006) found was for a relatively small catchment in Lushoto district. This relation is different in this study, because an image of the entire district was used in contrast to only a small portion, which means that different land use types might be present. Also, sun elevation and atmospheric conditions may differ from the image that Vrieling et al. (2006) used. It was assumed that the highest NDVI value in the Landsat ETM+ image corresponds to a fractional vegetation cover of 1, whereas the lowest NDVI value found on a land surface would (i.e. no water bodies) correspond to a fractional vegetation cover of 0. The following relation was then found and used to create a fractional vegetation cover (FVC) map:

$$FVC = 1.1841 * NDVI - 0.0093$$

Because the ASTER DEM does not cover the entire Lushoto district, a slope map was created using a contour lines map with a vertical accuracy of 50m which was done with ArcGis (version 10, ESRI, Redlands, California, USA). The DEM was converted into a slope map and divided into classes of 10% slope. This slope map in combination with the FVC map was used to create an erosion risk map using the decision tree developed by Vrieling et al. (2006). This decision tree is depicted in table A.1.

Table A.1 Decision tree for the construction of the erosion risk map (Vrieling et al., 2006)

FVC (%)		Slope (%)	Erosion risk
80-100		0-40	Very Low
80-100		>40	Low
60-80		0-30	Low
60-80		>30	Medium
40-60		0-10	Low
40-60	10-40	Medium	
40-60	>40	High	
20-40	0-10	Low	
20-40	10-20	Medium	
20-40	20-30	High	
20-40	>30	Very High	
0-20	0-10	Low	
0-20	10-20	High	
0-20	>20	Very High	

Figure A.1 shows the erosion risk map created from the NDVI of the ETM+ image and the DEM created from the contour lines. Erosion risk is especially high (red) at the edges of the mountain plateau where the altitudes go from 1800 m to 600 m over just hundreds of meters. Erosion is also high in the eastern part of the area where little vegetation is present and slopes are steep. In areas with a high NDVI like forested areas, such as the areas to the east and northwest of Lushoto, the erosion risk is low.

Figure A.2 shows the histogram for the erosion risk mapping of the entire Lushoto district. The majority of the area is classified as class 2 (low) and 3 (medium), which together account for 81% of the total area. Only 3% of the district belongs to the class 5, meaning a very high erosion risk.
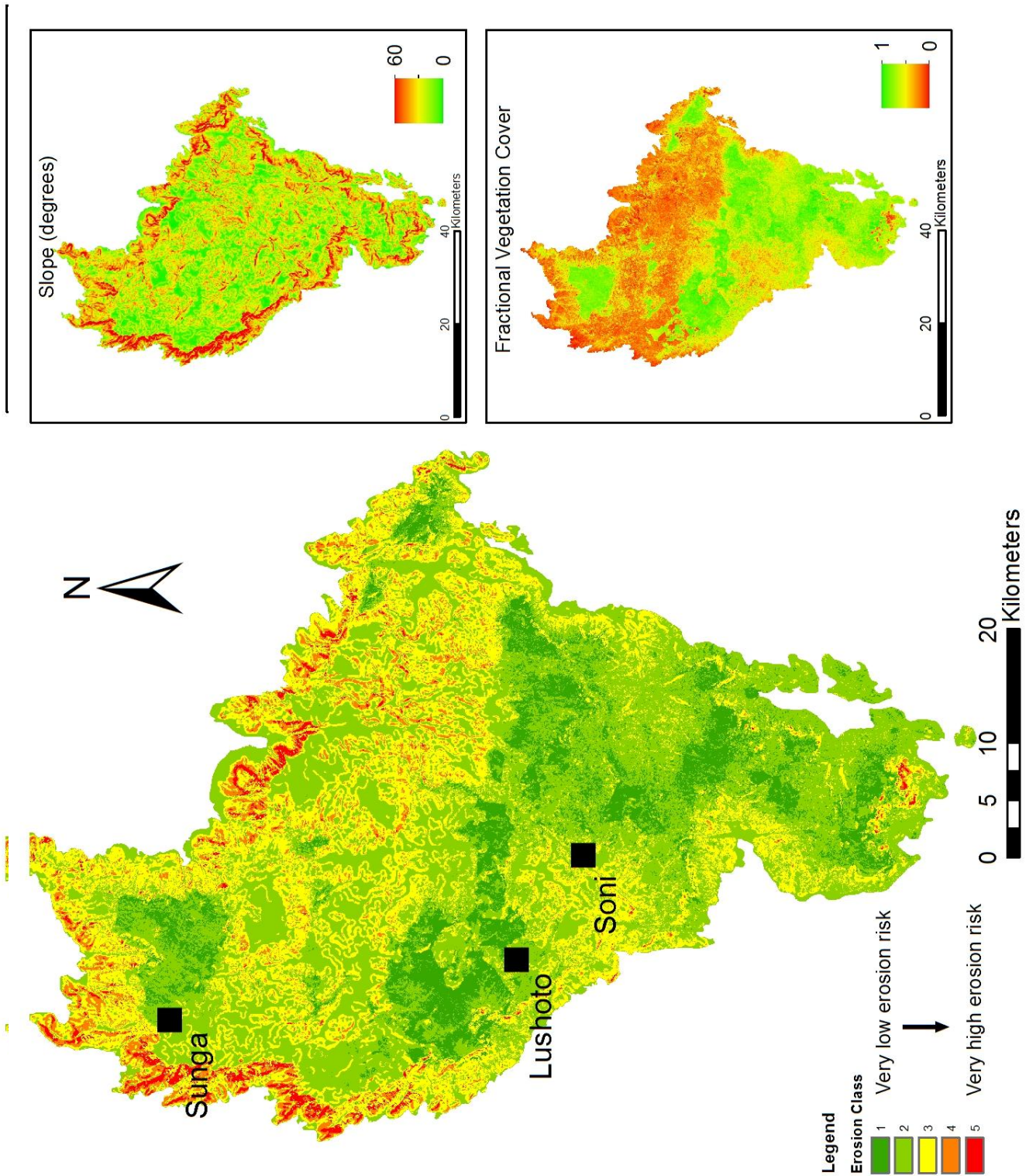
Figure A.1: Erosion Risk map of the Lushoto district, Tanzania created using a Landsat ETM+ image and a digital elevation model. Also shown are the fractional vegetation cover map and slope map that served as input for the Erosion risk map
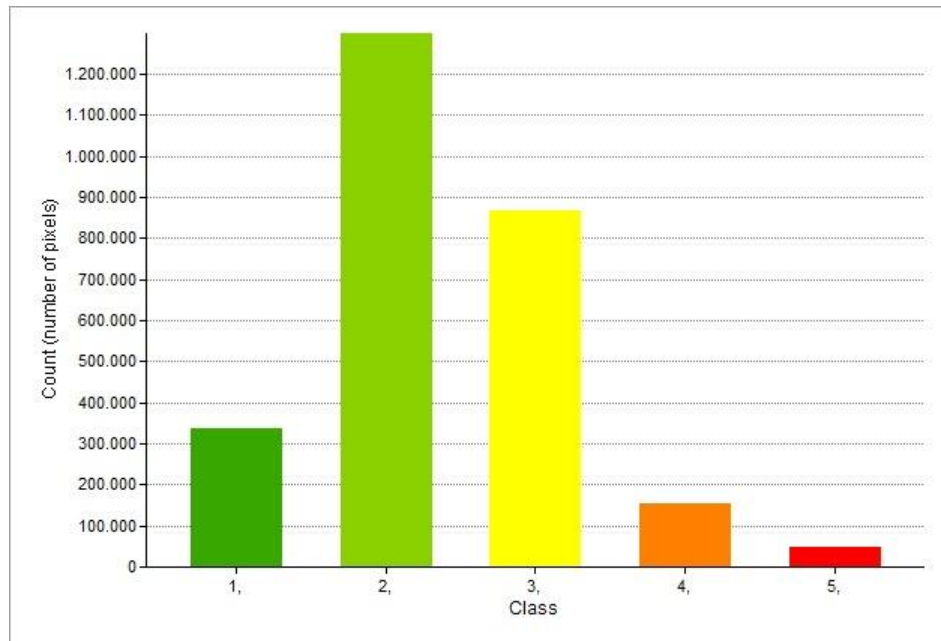
Figure A.2 Histogram for the erosion risk map of the entire Lushoto district, Tanzania. The number of pixels that belong to a certain erosion risk class (1=very low, 5=very high) are depicted.

The erosion risk map created using the ETM+ image and the DEM created from contour lines is only an indication where the most erosion risk might occur and is only dependent on slope and the cover by vegetation. The vegetation cover is determined by the NDVI, which is a snapshot in time. This means that with changing seasons, the erosion risk changes. In this case the NDVI was of October, which is at the end of a dry season. This means that erosion risk is relatively high for the time period which was used compared to other moments throughout the year.

Furthermore the actual erosion would depend on many other factors e.g. rainfall intensity and duration, maximum storage capacity of the vegetation, cohesion of the soil and the presence of soil and water conservation measures. In order to determine actual quantitative erosion in the entire area more accurate data is needed, ideally on a per-pixel basis, but this would be practically impossible.

Appendix II: DVD with used data and products.